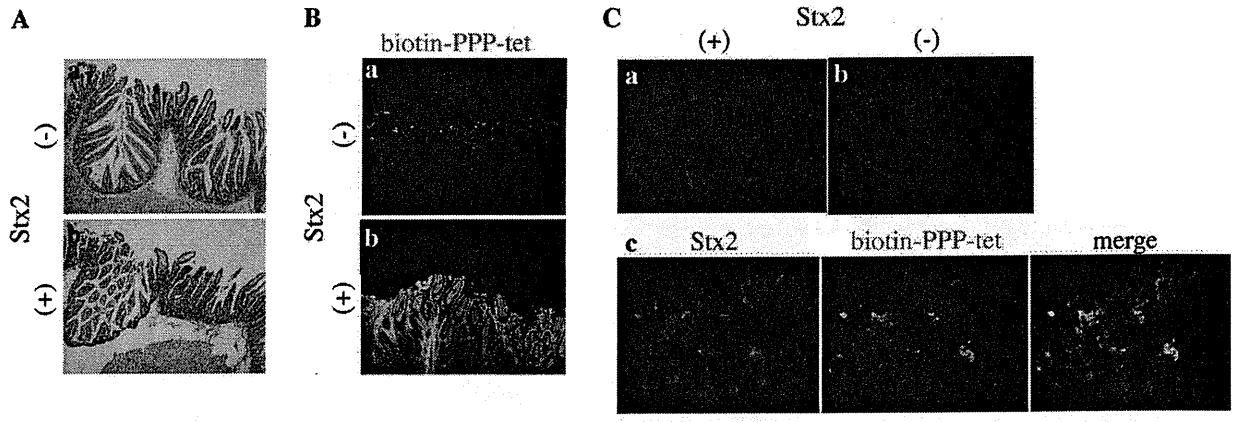

FIG. 3. Tetravalent peptides accumulate in the ileal epithelial cells in a complex with Stx2. (A) Hematoxylin and eosin staining of sections obtained from the ileal blocks. The blocks were treated with PBS (a) or Stx2 (10 μg/ml) (b) for 1 h. (B) Localization of biotin-PPP-tet by using streptavidin-Alexa 488. The block was treated with PBS (a) or Stx2 (10 μg/ml) (b) in the presence of biotin-PPP-tet (1.4 mM) for 1 h. (C) Colocalization of Stx2 and biotin-PPP-tet by using anti-Stx monoclonal antibody and streptavidin-Alexa 488. Images show blocks treated with Stx2 (10 μg/ml) (a) and PBS (b), as well as blocks treated with Stx2 (10 μg/ml) plus biotin-PPP-tet (1.4 mM) (c).

inhibit Stx2 cytotoxicity in ileal epithelial cells, we examined the effects of the peptides on the intracellular transport of the toxin by using Caco-2 cells, a human colon epithelial cell line. As shown in Fig. 4, Ac-PPP-tet efficiently protected Caco-2 cells against the cytotoxic effects of 100 pg/ml Stx2, which resulted in 50% cell viability after a 2-day incubation. Biotin-PPP-tet had a dose-dependent protective effect almost identical to that of Ac-PPP-tet (data not shown). Next, we analyzed the intracellular localization of Alexa Fluor 488-labeled Stx2 after its binding to the surface receptor on Caco-2 cells. Time-dependent localization of Stx2 to the Golgi apparatus was confirmed by colocalization with the Golgi apparatus marker GM130 (Fig. 5B). This localization pattern merged well with that of Alexa Fluor 555-labeled Ac-PPP-tet (Fig. 5A), suggesting that the peptide forms a complex with Stx2 and that this complex is then incorporated into the cells and transferred to the Golgi apparatus. In contrast, colocalization of Stx2 with the ER marker Hsp47 was completely inhibited by the presence of Ac-PPP-tet (Fig. 5C), indicating that the transport of Stx2 from the Golgi apparatus to the ER was specifically blocked by the presence of Ac-PPP-tet.

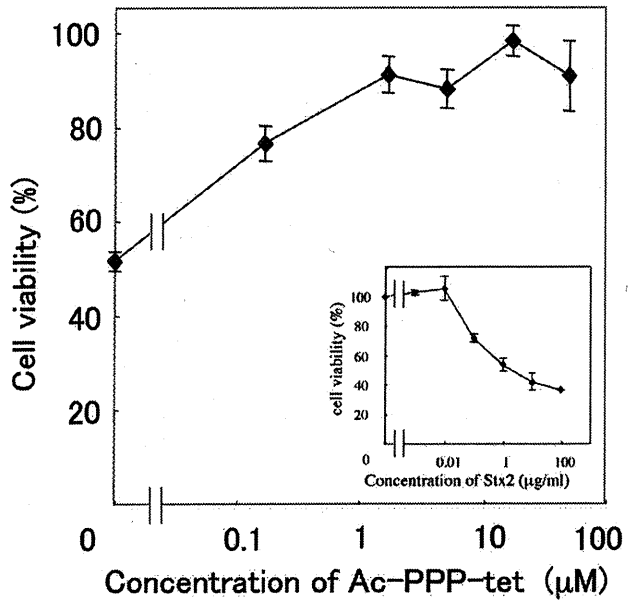

FIG. 4. Tetravalent peptides inhibit Stx2 cytotoxicity in Caco-2 cells. Caco-2 cells were treated with Stx2 (100 pg/ml) in the presence of Ac-PPP-tet for 48 h, and cell viability was determined. The inset shows the dose-dependent effects of Stx2 on Caco-2 cell viability. Data are expressed as percentages (means ± standard errors; $n = 3$) of the control value.

In order to further confirm the above conclusion, we examined whether Ac-PPP-tet could directly interact with Stx2 in living cells. After treatment of Caco-2 cells with Alexa Fluor 555-labeled Ac-PPP-tet, Ac-PPP-tet was substantially incorporated into and diffusely distributed in the cells. Following the addition of Alexa Fluor 488-labeled Stx2, Ac-PPP-tet was dynamically redistributed to the Golgi region, where it colocalized with Stx2 (Fig. 6). Such movement of Ac-PPP-tet was not observed in the absence of Stx2. These results indicate that Ac-PPP-tet can directly bind to Stx2 in living cells and that Stx2 is then transferred to the Golgi apparatus in a complex with Ac-PPP-tet.

DISCUSSION

In the present study, we found that Ac-PPP-tet completely inhibited fluid accumulation and tissue damage in the rabbit ileum caused by the direct injection of Stx2 when Ac-PPP-tet and the toxin were administered simultaneously. Since the rabbit ileal loop system is highly suitable for evaluating the direct toxicity of Stx2 in intestinal epithelial cells, our finding clearly demonstrates that Ac-PPP-tet functions to protect epithelial cells from damage caused by the toxin. Our findings also suggest that the tetravalent peptide accumulates in ileal epithelial cells only through the formation of a complex with Stx2. Thus, the mechanism of action of Ac-PPP-tet is likely to be different from that of other Stx neutralizers previously

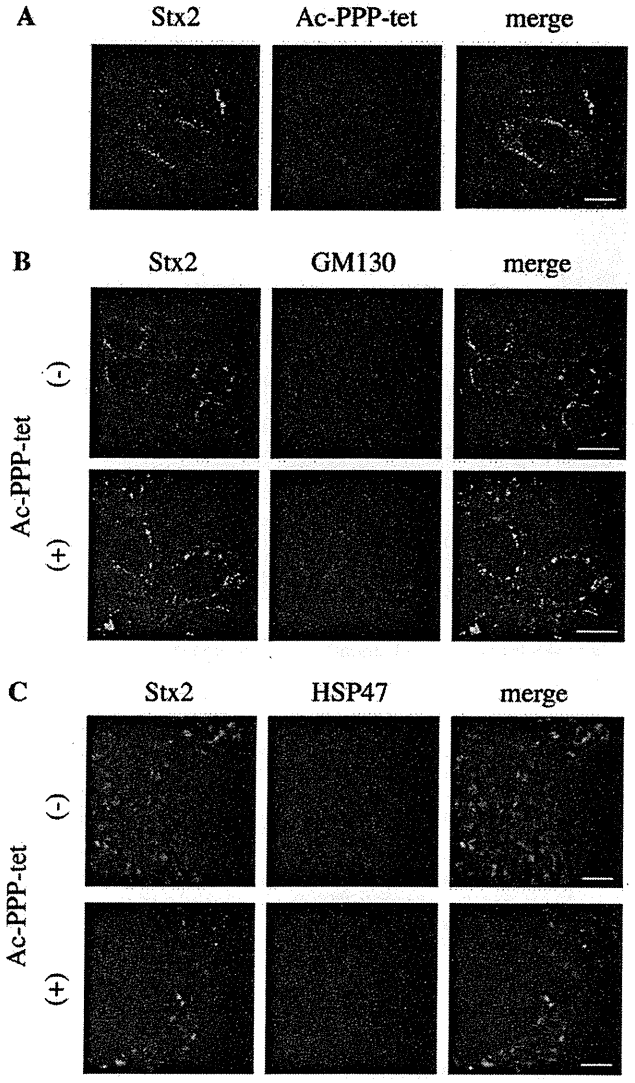

FIG. 5. Tetravalent peptides induce aberrant cellular transport of Stx2 in Caco-2 cells. (A) Confocal images of the intracellular localization patterns of Alexa Fluor 488-labeled Stx2 (1 μg/ml) in the presence of Alexa Fluor 555-labeled Ac-PPP-tet (16 μM). The bar indicates 20 μm. (B) Immunocytochemical analysis of the colocalization of Stx2 (1 μg/ml) with GM130 in the presence or absence of Ac-PPP-tet (49 μM). The bars indicate 20 μm. (C) Immunocytochemical analysis of the colocalization of Stx2 (1 μg/ml) with Hsp47 in the presence or absence of Ac-PPP-tet (49 μM). The bars indicate 5 μm.

shown to function in the intestinal tract, all of which exert their inhibitory effects by binding to the toxin and inhibiting its incorporation into the epithelial cells (24, 35, 36). In Caco-2 cells, the formation of complexes of Ac-PPP-tet and Stx2 blocked the intracellular transport of Stx2 from the Golgi apparatus to the ER, probably resulting in the efficient degradation of this toxin. Thus, Ac-PPP-tet appears to function in the intestine by affecting the intracellular transport of Stx2, confirming the crucial role of this transport system in vivo, especially in the intestinal epithelial cells.

In mice, Ac-PPP-tet offers remarkable protection against the lethality of *E. coli* O157:H7 infection when the peptide is administered intragastrically beginning on day 2 of infection (20). Interestingly, Stx was undetectable in sera from Ac-PPP-tet-treated mice on day 3 of infection, when serum Stx concentrations in untreated mice peaked (data not shown) (15). The molecular basis of this phenomenon is unclear, though the present findings suggest that intragastrically administered Ac-PPP-tet induces detoxification of Stx2 in the intestinal epithelial cells and, consequently, prevents its intrusion into the circulation. We have found that direct administration of Ac-PPP-tet into the circulation with Stx2 does not rescue mice from lethality (K. Nishikawa et al., unpublished data), supporting the notion that orally administered Ac-PPP-tet detoxifies Stx2 in the intestine but not in the circulation.

In Caco-2 cells, both Stx1 and Stx2 are transported to the ER along the retrograde pathway and inhibit protein synthesis (30). Stx1 is also able to translocate across the apical side of the intestinal epithelial monolayer to the basolateral side in a Gb3-independent manner. The ability of Stx2 to perform this type of translocation is approximately 10-fold weaker (1, 10). Thus, the fluid accumulation and tissue damage observed in the present study are likely attributable to Stx2, which is transported mainly through the retrograde pathway rather than through transcytosis across intestinal epithelial cells. Moreover, Ac-PPP-tet may protect against the Stx2-induced ileal damage by inhibiting the retrograde transport of the toxin.

We have previously shown that, in Caco-2 cells, the cell binding and retrograde transport of Stx1 and Stx2 are Gb3-dependent events. Specifically, we showed that Stx-stimulated interleukin-8 production, which requires transport of the catalytic A subunit into the cytosol through the retrograde pathway, is markedly inhibited by SUPER TWIGs (37; Nishikawa et al., unpublished), synthetic Stx neutralizers that contain the trisaccharide moiety of Gb3 in multivalent configurations (19). Given that Ac-PPP-tet specifically binds to Stx2 through one of the three trisaccharide-binding sites on the B subunit (site 3), our present observations suggest that the Stx2–Ac-PPP-tet complex binds to cell surface Gb3 through the remaining binding site(s) (i.e., site 1 and/or site 2) and is then transferred to the Golgi apparatus but not to the ER in Caco-2 cells. Taken together, our findings support an essential role for site 3 in the transport of Stx2 from the Golgi apparatus to the ER in the ileal epithelial cells, as has been shown previously for Vero cells (20).

A high-molecular-weight fraction of hop bract extract (HBT), which contains procyanidine polymers, has been shown previously to inhibit the cytotoxic activity of Stx1 in Vero cells and Stx1-induced fluid accumulation in the rabbit ileal loop (32). HBT inhibits the RNA *N*-glycosidase activity of the Stx1 A subunit and then interferes with protein synthesis inhibition, suggesting that the direct target of HBT is the catalytic A subunit of Stx. On the other hand, the Stx2 B subunit has been shown to induce fluid accumulation independently of A subunit activity in rat colon loops by altering the balance of intestinal absorption and secretion toward net secretion (4). Thus, the potent inhibitory effect of Ac-PPP-tet on Stx2-induced fluid accumulation in rabbit ileal loops may be attributable to the unique ability of Ac-PPP-tet to inhibit not only the cytotoxicity of the A subunit by inducing aberrant transport and degradation, but also A subunit-independent intracellular signaling

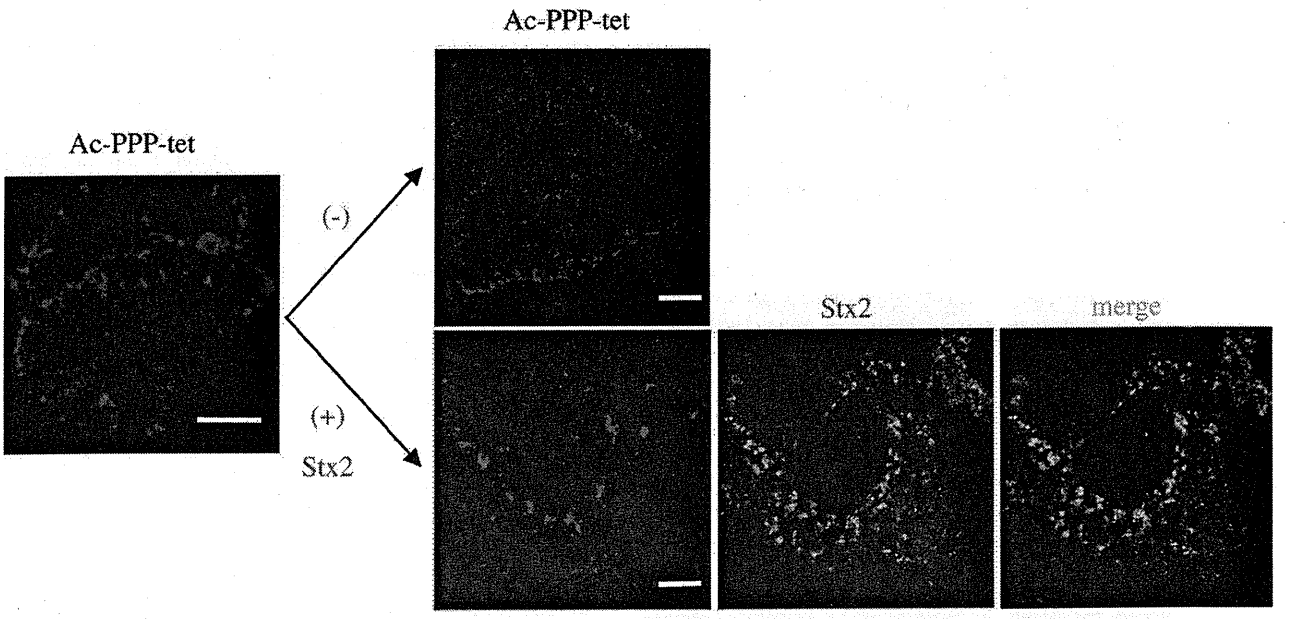

FIG. 6. Complex formation by Ac-PPP-tet and Stx2 in Caco-2 cells. Caco-2 cells that were pretreated with Alexa Fluor 555-labeled Ac-PPP-tet (16 μM) were cultured for 30 min in the presence or absence of Alexa Fluor 488-labeled Stx2 (1 μg/ml). Confocal images of the intracellular localization patterns of Ac-PPP-tet and Stx2 are shown. The bars indicate 10 μm.

activated by the B subunit through binding with Gb3. Previous observations that the protein kinase C inhibitor H-7 and indomethacin inhibit Stx1-induced fluid accumulation in the rabbit ileum without directly affecting the toxin (13) suggest that protein kinase C activation and prostaglandin production participate in signaling downstream of the binding of Stx with Gb3. Similar intracellular signaling events may be blocked by the formation of complexes between Stx2 and Ac-PPP-tet in epithelial cells, although this issue awaits further investigation.

In conclusion, our results suggest that orally administered Ac-PPP-tet accumulates in ileal epithelial cells through the formation of a complex with Stx2. Formation of this complex may specifically block the intracellular transport of Stx2 from the Golgi apparatus to the ER, resulting in the degradation of the toxin and a reduction in its circulating levels. Thus, Ac-PPP-tet appears to function in the intestine by affecting the intracellular transport of Stx2 in the epithelial cells.

ACKNOWLEDGMENTS

We thank Michael Berne (Tufts University) for peptide synthesis.

This study was supported by an International Health Cooperation Research grant (18-C-5) from the Ministry of Health, Labor and Welfare, Japan; a grant from the Fugaku Trust for Medicinal Research; and grants from the Ministry of Education, Culture, Sports, Science and Technology, Japan (an Academic Frontier Research Project grant for the "New Frontier of Biomedical Engineering Research" and scientific research grant no. 19659027).

REFERENCES

1. **Acheson, D. W., R. Moore, S. De Breucker, L. Lincicome, M. Jacewicz, E. Skutelsky, and G. T. Keusch.** 1996. Translocation of Shiga toxin across polarized intestinal cells in tissue culture. Infect. Immun. **64:**3294–3300.
2. **Arab, S., and C. A. Lingwood.** 1998. Intracellular targeting of the endoplasmic reticulum/nuclear envelope by retrograde transport may determine cell hypersensitivity to verotoxin via globotriaosyl ceramide fatty acid isoform traffic. J. Cell. Physiol. **177:**646–660.
3. **Armstrong, G. D., E. Fodor, and R. Vanmaele.** 1991. Investigation of Shiga-like toxin binding to chemically synthesized oligosaccharide sequences. J. Infect. Dis. **164:**1160–1167.
4. **Creydt, V. P., M. F. Miyakawa, F. Martín, E. Zotta, C. Silberstein, and C. Ibarra.** 2004. The Shiga toxin 2 B subunit inhibits net fluid absorption in human colon and elicits fluid accumulation in rat colon loops. Braz. J. Med. Biol. Res. **37:**799–808.
5. **Dohi, H., Y. Nishida, M. Mizuno, M. Shinkai, T. Kobayashi, T. Takeda, H. Uzawa, and K. Kobayashi.** 1999. Synthesis of an artificial glycoconjugate polymer carrying Pk-antigenic trisaccharide and its potent neutralization activity against Shiga-like toxin. Bioorg. Med. Chem. **7:**2053–2062.
6. **Donohue-Rolfe, A., I. Kondova, S. Oswald, D. Hutto, and S. Tzipori.** 2000. Escherichia coli O157:H7 strains that express Shiga toxin (Stx) 2 alone are more neurotropic for gnotobiotic piglets than are isotypes producing only Stx1 or both Stx1 and Stx2. J. Infect. Dis. **181:**1825–1829.
7. **Fraser, M. E., M. Fujinaga, M. M. Cherney, A. R. Melton-Celsa, E. M. Twiddy, A. D. O'Brien, and M. N. James.** 2004. Structure of Shiga toxin type 2 (Stx2) from Escherichia coli O157:H7. J. Biol. Chem. **279:**27511–27517.
8. **Gorbach, S. L., J. G. Banwell, B. D. Chatterjee, B. Jacobs, and R. B. Sack.** 1971. Acute undifferentiated human diarrhea in the tropics. I. Alterations in intestinal micrflora. J. Clin. Invest. **50:**881–889.
9. **Hitotsubashi, S., Y. Fujii, H. Yamanaka, and K. Okamoto.** 1992. Some properties of purified *Escherichia coli* heat-stable enterotoxin II. Infect. Immun. **60:**4468–4474.
10. **Hurley, B. P., M. Jacewicz, C. M. Thorpe, L. L. Lincicome, A. J. King, G. T. Keusch, and D. W. Acheson.** 1999. Shiga toxins 1 and 2 translocate differently across polarized intestinal epithelial cells. Infect. Immun. **67:**6670–6677.
11. **Karmali, M. A., M. Petric, C. Lim, P. C. Fleming, G. S. Arbus, and H. Lior.** 1985. The association between idiopathic hemolytic uremic syndrome and infection by verotoxin-producing *Escherichia coli*. J. Infect. Dis. **151:**775–782.
12. **Karmali, M. A., B. T. Steele, M. Petric, and C. Lim.** 1983. Sporadic cases of hemolytic uremic syndrome associated with fecal cytotoxin and cytotoxin-producing *Escherichia coli*. Lancet **1:**619–620.
13. **Kaur, T., S. Singh, M. Verma, and N. K. Ganguly.** 1997. Calcium and protein kinase C play a significant role in response to Shigella toxin in rabbit ileum both in vivo and in vitro. Biochim. Biophys. Acta **1361:**75–91.
14. **Kitov, P. I., J. M. Sadowska, G. Mulvey, G. D. Armstrong, H. Ling, N. S. Pannu, R. J. Read, and D. R. Bundle.** 2000. Shiga-like toxins are neutralized by tailored multivalent carbohydrate ligands. Nature **403:**669–672.
15. **Kurioka, T., Y. Yunou, and E. Kita.** 1998. Enhancement of susceptibility to Shiga toxin-producing *Escherichia coli* O157:H7 by protein calorie malnutrition in mice. Infect. Immun. **66:**1726–1734.
16. **Ling, H., A. Boodhoo, B. Hazes, M. D. Cummings, G. D. Armstrong, J. L. Brunton, and R. J. Read.** 1998. Structure of the Shiga-like toxin I B-penta-

mer complexed with an analogue of its receptor Gb_3. Biochemistry **37:**1777–1788.
17. **Melton-Celsa, A. R., and A. D. O'Brien.** 1998. Structure, biology, and relative toxicity of Shiga toxin family members for cells and animals, p. 121–128. *In* J. B. Kaper and A. D. O'Brien (ed.), *Escherichia coli* O157:H7 and other Shiga toxin-producing *E. coli* strains. American Society for Microbiology, Washington, DC.
18. **Mulvey, G. L., P. Marcato, P. I. Kitov, J. Sadowska, D. R. Bundle, and G. D. Armstrong.** 2003. Assessment in mice of the therapeutic potential of tailored, multivalent Shiga toxin carbohydrate ligands. J. Infect. Dis. **187:**640–649.
19. **Nishikawa, K., K. Matsuoka, E. Kita, N. Okabe, M. Mizuguchi, K. Hino, S. Miyazawa, C. Yamasaki, J. Aoki, S. Takashima, Y. Yamakawa, M. Nishijima, D. Terunuma, H. Kuzuhara, and Y. Natori.** 2002. A therapeutic agent with oriented carbohydrates for treatment of infections by Shiga toxin-producing Escherichia coli O157:H7. Proc. Natl. Acad. Sci. U. S. A. **99:**7669–7674.
20. **Nishikawa, K., M. Watanabe, E. Kita, K. Igai, K. Omata, M. B. Yaffe, and Y. Natori.** 2006. A multivalent peptide-library approach identifies a novel Shiga toxin-inhibitor that induces aberrant cellular transport of the toxin. FASEB J. **20:**2597–2599.
21. **Noda, M., T. Yutsudo, N. Nakabayashi, T. Hirayama, and Y. Takeda.** 1987. Purification and some properties of Shiga-like toxin from *Escherichia coli* O157:H7 that is immunologically identical to Shiga toxin. Microb. Pathog. **2:**339–349.
22. **O'Brien, A. D., and R. K. Holmes.** 1987. Shiga and Shiga-like toxins. Microbiol. Rev. **51:**206–220.
23. **Ostroff, S. M., P. I. Tarr, M. A. Neill, J. H. Lewis, N. Hargrett-Bean, and J. M. Kobayashi.** 1989. Toxin genotypes and plasmid profiles as determinants of systemic sequelae in Escherichia coli O157:H7 infections. J. Infect. Dis. **160:**994–998.
24. **Paton, A. W., R. Morona, and J. C. Paton.** 2000. A new biological agent for treatment of Shiga toxigenic Escherichia coli infections and dysentery in humans. Nat. Med. **6:**265–270.
25. **Paton, J. C., and A. W. Paton.** 1998. Pathogenesis and diagnosis of Shiga toxin-producing *Escherichia coli* infections. Clin. Microbiol. Rev. **11:**450–479.
26. **Riley, L. W., R. S. Remis, S. D. Helgerson, H. B. McGee, J. G. Wells, B. R. Davis, R. J. Hebert, E. S. Olcott, L. M. Johnson, N. T. Hargrett, P. A. Blake, and M. L. Cohen.** 1983. Hemorrhagic colitis associated with a rare *Escherichia coli* serotype. N. Engl. J. Med. **308:**681–685.
27. **Sandvig, K., O. Garred, K. Prydz, J. V. Kozlov, S. H. Hansen, and B. van Deurs.** 1992. Retrograde transport of endocytosed Shiga toxin to the endoplasmic reticulum. Nature **358:**510–512.
28. **Sandvig, K., M. Ryd, O. Garred, E. Schweda, P. K. Holm, and B. van Deurs.** 1994. Retrograde transport from the Golgi complex to the ER of both Shiga toxin and the nontoxic Shiga B-fragment is regulated by butyric acid and cAMP. J. Cell Biol. **126:**53–64.
29. **Sandvig, K., and B. van Deurs.** 2000. Entry of ricin and Shiga toxin into cells: molecular mechanisms and medical perspectives. EMBO J. **19:**5943–5950.
30. **Schüller, S., G. Frankel, and A. D. Phillips.** 2004. Interaction of Shiga toxin from Escherichia coli with human intestinal epithelial cell lines and explants: Stx2 induces epithelial damage in organ culture. Cell. Microbiol. **6:**289–301.
31. **Siegler, R. L., T. G. Obrig, T. Pysher, J., V. L. Tesh, N. D. Denkers, and F. B. Taylor.** 2003. Response to Shiga toxin 1 and 2 in a baboon model of hemolytic uremic syndrome. Pediatr. Nephrol. **18:**92–96.
32. **Tagashira, M., K. Yahiro, N. Morinaga, J. Moss, and M. Noda.** 2003. Protection with hop bract polyphenol of mice infected with enterohemorrhagic *Escherichia coli* O157:H7 through inhibition of Shiga toxin-1 toxicity. p. 45–48. *In* 38th U.S.-Japan Cholera and Other Bacterial Enteric Infections Joint Panel Meeting. U.S. Department of Health and Human Disease, Public Health Service, National Institutes of Health, Bethesda, MD.
33. **Tesh, V. L., J. A. Burris, J. W. Owens, V. M. Gordon, E. A. Wadolkowski, A. D. O'Brien, and J. E. Samuel.** 1993. Comparison of the relative toxicities of Shiga-like toxins type I and type II for mice. Infect. Immun. **61:**3392–3402.
34. **Uesaka, Y., Y. Otsuka, Z. Lin, S. Yamasaki, J. Yamaoka, H. Kurazono, and Y. Takeda.** 1994. Simple method of purification of Escherichia coli heat-labile enterotoxin and cholera toxin using immobilized galactose. Microb. Pathog. **16:**71–76.
35. **Watanabe, M., K. Igai, K. Matsuoka, A. Miyagawa, T. Watanabe, R. Yanoshita, Y. Samejima, D. Terunuma, Y. Natori, and K. Nishikawa.** 2006. Structural analysis of the interaction between Shiga toxin B-subunits and linear polymers bearing clustered globotriose residues. Infect. Immun. **74:**1984–1988.
36. **Watanabe, M., K. Matsuoka, E. Kita, K. Igai, N. Higashi, A. Miyagawa, T. Watanabe, R. Yanoshita, Y. Samejima, D. Terunuma, Y. Natori, and K. Nishikawa.** 2004. Oral therapeutic agents with highly clustered globotriose for treatment of Shiga toxigenic Escherichia coli infections. J. Infect. Dis. **189:**360–368.
37. **Yamasaki, C., Y. Natori, X.-T. Zeng, M. Ohmura, S. Yamasaki, Y. Takeda, and Y. Natori.** 1999. Induction of cytokines in a human colon epithelial cell line by Shiga toxin 1 (Stx1) and Stx2 but not by non-toxic mutant Stx1 which lacks *N*-glycosidase activity. FEBS Lett. **442:**231–234.

Editor: J. B. Bliska

FULL PAPER *Bacteriology*

Distribution of Virulence Genes Related to Adhesins and Toxins in Shiga Toxin-Producing *Escherichia coli* Strains Isolated from Healthy Cattle and Diarrheal Patients in Japan

Yuluo WU[1)], Atsushi HINENOYA[1)], Takashi TAGUCHI[1)], Akira NAGITA[2)], Kensuke SHIMA[1)], Teizo TSUKAMOTO[1)], Norihiko SUGIMOTO[1)], Masahiro ASAKURA[1)] and Shinji YAMASAKI[1)]*

[1)]*Graduate School of Life and Environmental Sciences, Osaka Prefecture University, Osaka, 598-8531 and* [2)]*Department of Pediatrics, Mizushima Central Hospital, Okayama, 712-8064, Japan*

(Received 10 December 2009/Accepted 12 January 2010/Published online in J-STAGE 26 January 2010)

ABSTRACT. Shiga toxin-producing *Escherichia coli* (STEC) isolated from Japan were investigated for the distribution of virulence genes. A total of 232 STEC strains including 171 from cattle and 61 from human were examined for the occurrence of genes responsible for bacterial adhesions to intestine, e.g., *eae* (intimin, *E. coli* attaching and effacing), *saa* (STEC autoagglutinating adhesin), *iha* (*irgA* homologue adhesin), *efa1* (*E. coli* factor for adherence), $lpfA_{O113}$ (long polar fimbriae), and *ehaA* (EHEC autotransporter) by colony hybridization assay. Similarly, the presence of toxigenic *cdt* (cytolethal distending toxin), and *subAB* (subtilase cytotoxin) genes were also checked. Among cattle isolates, 170, 163, 161, 155, 112 and 84 were positive for $lpfA_{O113}$ (99%), *ehaA* (95%), *iha* (94%), *saa* (91%), *subAB* (65%), and *cdt-V* (49%), respectively, while 2 were positive for *eae* (1.2%) and *efa1* (1.2%) each. In case of human isolates, 60, 59, 58 and 58 were positive for *ehaA* (98%), *iha* (97%), *efa1* (95%), and *eae* (95%), respectively, while 11, 2, 2, and 1 were positive for $lpfA_{O113}$ (18%), *saa* (3.3%), *cdt-V* (3.3%), and *subAB* (1.6%), respectively. Therefore, in human STEC isolates *efa1* and *eae* whereas in cattle isolates *saa*, $lpfA_{O113}$, *cdt-V* and *subAB* were prevalent. These data indicate differential occurrence of some pathogenic genes in human and cattle originated STEC strains in Japan.

KEY WORDS: bacterial toxin, cattle, *E. coli* infection, molecular epidemiology, virulence genes.

J. Vet. Med. Sci. 72(5): 589–597, 2010

Shiga toxin-producing *Escherichia coli* (STEC), also called Vero toxin (VT)-producing *E. coli* (VTEC) or eneterohemorrhagic *E. coli* (EHEC), are known to cause acute gastroenteritis, hemorrhagic colitis (HC) and hemolytic-uremic syndrome (HUS) in humans [30, 43]. Since the occurrence of first food poisoning due to EHEC infection in 1982, sporadic cases and outbreaks have been reported in many countries including Japan [3, 18, 21, 40, 43]. The Japanese government has initiated a national surveillance for EHEC infections since 1991 when 2 children died due to EHEC O157:H7 infection. In Japan, a yearly average of approximately 3,000 cases including symptomatic patients and asymptomatic carrier has been reported after 1996 when the largest outbreak of EHEC O157:H7 infection occurred in Sakai [21, 22]. During 2007-2008, the yearly average of EHEC cases in Japan increased to more than 4,000 [22]. In the US, however, it is estimated that STEC is responsible for approximately 100,000 illness, 3,000 hospitalization, and 90 death annually [20].

Cattle and other ruminants have been implicated as primary reservoirs of STEC O157:H7 as well as non-O157 STEC [8, 16, 17]. Previous studies estimated that about 28% cattle secrete STEC O157:H7 in their feces in the US [6]. Therefore, consumption of raw beef and undercooked meat could be a source of STEC infection [8, 30, 43]. However, sporadic cases and outbreaks of STEC infection due to consumption of vegetable, fruit and other daily dish have also been reported. There are also considerable cases of person-to-person transmission of STEC infection [8, 30, 43].

Shiga toxin (Stx), divided into 2 groups such as Stx1 and Stx2, is the most important virulence factors in STEC [43]. Although more than 400 serotypes of *E. coli* which produce Stx1 and/or Stx2 have been isolated from cattle, serotype O157:H7 has been frequently isolated from patients with gastroenteritis [8]. Usually, STEC strains belonging to serogroups O157, O26, and O111 produce attaching and effacing (A/E) lesions on intestinal mucosa, which are mediated by the locus of enterocyte effacement (LEE) pathogenicity island [30]. The LEE containing *eae* gene codes for an outer membrane protein, called intimin, which is responsible for intimate attachment of the bacteria to the host intestinal cells [19]. Intimin has been classified into at least 10 different types (α to κ) on the basis of variability of its C-terminal region. It has been suggested that differences in amino acid sequences of the intimin proteins influence the pattern of colonization and tissue tropism in the host [39, 44]. Most of the STEC strains isolated from patients with HC and HUS belonged to specific serogroups also contain LEE [30].

However, LEE-negative STEC strains belonging to other serogroups besides O157, O26 and O111 have also been isolated from patients not only with gastroenteritis but also with HUS [1, 28]. Therefore a tremendous effort has been made to discover adherence factors other than intimin. As a result, Saa (STEC autoagglutinating adhesin) [27], $LpfA_{O113}$

* CORRESPONDENCE TO: YAMASAKI, S., Graduate School of Life and Environmental Sciences, Osaka Prefecture University, 1-58 Rinkuourai-Kita, Izumisano, Osaka 598-8531, Japan.
e-mail : shinji@vet.osakafu-u.ac.jp

(long polar fimbriae) [5], Efa1 (EHEC factor for adherence) [23], Iha (*Vibrio cholerae* IrgA homologue adhesin) [33], EhaA (EHEC autotransporter) [36] etc., which are not encoded by the LEE region, have been identified in both LEE-negative and LEE-positive STEC strains. Furthermore, genes encoding cytolethal distending toxin (CDT) [13] and subtilase cytotoxin (SubAB) [28] have also been identified in LEE-positive and LEE-negative STEC strains, respectively. Although the prevalence of genes encoding putative adhesins and newly identified toxins have been reported in STEC strains isolated from a limited geographic area [4, 15, 29, 37], very little is known about the distribution of such virulence-related genes in STEC strains isolated in Japan.

In this study, we examined the distribution of various virulence genes related to putative adhesion and newly identified toxins such as *cdt* and *subAB* among STEC strains isolated in Japan. Virulence gene profile of STEC strains was also compared between isolates from healthy cattle and human patients.

MATERIALS AND METHODS

STEC strains isolated from healthy cattle: A total of 171 Shiga toxin-producing *E. coli* (STEC) strains isolated from healthy cattle were analyzed in this study. These isolates were obtained by screening of 919 fecal samples collected from 61 healthy cattle in several pens in a barn every two weeks from February 2005 to January 2006 [Taguchi, T. *et al.*, unpublished data]. Aliquot of stool specimens was inoculated in 3 m*l* of tryptic soy broth (TSB) (Becton Dickinson, Franklin Lakes, NJ, U.S.A.) at 37°C overnight. Hundred micro liter of the culture was added into 900 μl of TE buffer (10 mM Tris-HCl, 1 mM EDTA [pH 8.0]) and boiled for 10 min. After centrifugation, the supernatant was used for PCR assay. The *stx1* and *stx2* genes were detected by multiplex-PCR assay as described previously [25] (Table 1). The overnight cultures, which were positive for *stx* genes, were serially diluted with 10 mM phosphate-buffered saline (pH 7.0) (PBS) and 100 μl of each dilution was spread on MacConkey agar (Becton Dickinson) plates. The colonies were transferred to nitrocellulose membrane (Schleicher & Schuell, Dassel, Germany) by a replica blotting method and a colony hybridization assay was carried out under high-stringent condition (50% formamide in hybridization buffer and 65°C incubation for washing) by using ^{32}P-labeled *stx1* or *stx2* gene as a probe as described previously [41]. For

Table 1. List of the primers and PCR conditions used in this study

Primer	Sequence (5'-3')	PCR conditions			Amplicon (bp)	Target gene	Reference
		Denaturing	Annealing	Extension			
EVT-1	CAACACTGGATGATCTCAG	94°C, 30 s	55°C, 30 s	72°C, 60 s	349	*stx1*	25
EVT-2	CCCCCTCAACTGCTAATA						
EVS-1	ATCAGTCGTCACTCACTGGT	94°C, 30 s	55°C, 30 s	72°C, 60 s	110	*stx2*	25
EVC-2	CTGCTGTCACAGTGACAAA						
EAE 1	AAACAGGTGAAACTGTTGCC	94°C, 60 s	55°C, 90 s	72°C, 90 s	454	*eaeA*	41
EAE 2	CTCTGCAGATTAACCTCTGC						
Saa-11	ACCTTCATGGCAACGAG	94°C, 30 s	55°C, 60 s	72°C, 90 s	1,504	*saa*	This study
Saa-22	AATGGACATGCCTGTGG						
Iha-u	GAAATCAGCATCCGAGG	94°C, 30 s	55°C, 30 s	72°C, 60 s	410	*iha*	This study
Iha-d	ATACGCGTGGCTGCTG						
Efa1-u	GTCAAAGGTGTTACAGAG	94°C, 30 s	55°C, 30 s	72°C, 60 s	640	*efaA1*	This study
Efa1-d	ATTCCATCCATCAGGCC						
LpfAO113-u	ACTTGTGAAGTTACCTCC	94°C, 30 s	55°C, 30 s	72°C, 60 s	360	$lpfA_{O113}$	This study
LpfAO113-d	CGGTATAAGCAGAGTCG						
EhaA-u	AGGCATGAGACACGATC	94°C, 30 s	55°C, 30 s	72°C, 60 s	500	*ehaA*	This study
EhaA-d	AAGTCGTGCCATTGAGC						
CdtB-commonF	TAAATGGAATATACATGTCCG	94°C, 30 s	50°C, 30 s	72°C, 60 s	588	*cdt-IB-VB*	10
CdtB-commonR	TTTCCAGCTACTGCATAATC						
P2-A2	CACTGACAACGGCTGAAC	94°C, 30 s	55°C, 30 s	72°C, 60 s	848	Upstream	10
cdtA-F	AAATGGGGAGCAGGATAC					of *cdt-VA*	
cdtC-F	CACTGACAACGGCTGAAC	94°C, 30 s	55°C, 30 s	72°C, 60 s	712	Downstream	10
P2-C3	AAATGGGGAGCAGGATAC					of *cdt-VC*	
Cdt-IBF	GATTTTGCCGGGTATTTCT	94°C, 30 s	50°C, 30 s	72°C, 60 s	700	*cdt-IB*	10
Cdt-IBR	CCCTCAACAGAGGAAGAA						
Cdt-IIIBF	TGTGCAGGAGGCAGGT	94°C, 30 s	50°C, 30 s	72°C, 60 s	490	*cdt-IIIB*	10
Cdt-IIIBR	TTGTGTCGGTGCAGCA						
Cdt-IVBF	TACCATCTTCAGCTACAC	94°C, 30 s	50°C, 30 s	72°C, 60 s	298	*cdt-IVB*	10
Cdt-IVBR	GCTCCAGAATCTATACCT						
eae-F	AGGATATTCTTTCTCTGAATA	95°C, 30 s	57°C, 30 s	72°C, 60 s	1,300	*eae*	39
eae-R	ATATYTATTTGCWGSVCCCCAT						
SubAF	GTACGGACTAACAGGGAACTG	94°C, 30 s	55°C, 30 s	72°C, 60 s	1,264	*subAB*	29
SubAR	ATCGTCATATGCACCTCCG						

Y, indicates T or C; W indicates A or T; S indicates G or C; V indicates G, C or A

Table 2. Distribution of genes of putative adhesins and other toxins in Shiga toxin-producing *Escherichia coli* strains isolated from cattle in Japan

PFGE[a] cluster	Serotype	No. of isolates	*stx* type	Adhesins						Other toxins	
				eae	*saa*	*iha*	*efa1*	*lpfA*$_{O113}$	*ehaA*	*cdt-V*	*subAB*
A	O130:H24	30	2	-	+	+	-	+	+	-	+
B	O163:H19	5	2	-	+	+	-	+	+	-	+
C	O17:H11	24	2	-	+	+	-	+	+	+	+
D	O113:NM[b]	17	2	-	+	+	-	+	+	+	+
E	O22:H8	43	1/2[d]	-	+	+	-	+	+	+	-
F	O153:H25	24	1/2	-	+	+	-	+	+	-	+
G	O40:HUT[c]	12	2	-	+	+	-	+	+	-	+
H	OUT:H16	7	2	-	-	-	-	+	-	-	-
I	O156:NM	4	2	-	-	+	-	+	+	-	-
J	O2:HUT	2	2	-	-	-	-	+	+	-	-
K	Orough:NM	1	1/2	-	-	+	-	-	-	-	-
L	O26:H11	1	1	+ (β)	-	+	+	+	+	-	-
M	O111:NM	1	1	+ (γ2)	-	-	+	+	+	-	-
	Total	171		2	155	161	2	170	163	84	112

a) Based on Tenover's criteria.
b) Nonmotile.
c) Untypable.
d) Both *stx1* and *stx2* positive.

Table 3. Distribution of genes of putative adhesins and other toxins in Shiga toxin-producing *Escherichia coli* strains isolated from patients in Japan

Isolation year	Serotype	No. of isolates	*stx* type	Adhesins						Other toxins	
				eae	*saa*	*iha*	*efa1*	*lpfA*$_{O113}$	*ehaA*	*cdt-V*	*subAB*
2000s	O157:H7	17	2	+ (γ1)	-	+	+	-	+	-	-
		3	1/2[c]	+	-	+	+	-	+	-	-
	O157:NM[a]	1	2	+	-	+	+	-	+	-	-
	O26:H11	3	2	+ (β)	-	+	+	+	+	-	-
	O111:NM	1	1/2	+ (γ2)	-	+	+	+	+	-	-
	O91:H21	1	2	-	+	+	-	+	+	+	-
	OUT[b]:NM	1	2	-	-	+	-	-	-	-	-
	Orough:H21	1	2	-	+	+	-	+	+	+	+
1990s	O157:H7	3	1	+ (γ1)	-	+	+	-	+	-	-
		4	2	+	-	+	+	-	+	-	-
		19	1/2	+	-	+	+	-	+	-	-
		1	1/2	+	-	-	+	-	+	-	-
	O26:H11	1	1	+ (β)	-	+	+	+	+	-	-
	O111:NM	1	1	+ (γ2)	-	-	+	+	+	-	-
		2	2	+	-	+	+	+	+	-	-
		1	1/2	+	-	+	+	+	+	-	-
	O145:NM	1	1	+ (γ1)	-	+	+	-	+	-	-
	Total	61		58	2	59	58	11	60	2	1

a) Nonmotile.
b) Untypable.
c) Both *stx1* and *stx2* positive.

stx1- and *stx2*-specific gene probes, an internal 0.9-kb *Hin*cII-*Hpa*I fragment of the *stx1* gene [41] and an internal 0.86-kb *Pst*I-*Sma*I fragment of the A subunit of the *stx2* gene were used, respectively. These fragments were labeled by the random priming method by using Multiprime DNA Labeling System (Amersham Biosciences Corp. Piscataway, NJ, U.S.A.) and [α-^{32}P]dCTP (111 TBq mmol^{-1} PerkinElmer, Waltham, MA, U.S.A.). The *stx1* and/or *stx2* gene-positive colonies were subcultured and confirmed as *E. coli* by conventional biochemical tests.

STEC strains isolated from diarrheal patients: A total of 1,771 rectal swabs were randomly collected from diarrheal patients who visited the pediatric department in Mizushima Central Hospital, Okayama from July 2004 to January 2009. Patient swab was suspended and enriched in 3 m*l* of TSB (Becton Dickinson) at 37°C overnight. STEC strains were

isolated as described above. Besides rectal swab samples, additional 33 STEC strains isolated in 1990s from our laboratory collection were also included in this study (Table 3).

Serotype: The serotype of the STEC strains were determined by tube agglutination with somatic (O1-O173) and flagellar (H1-H56) antisera prepared at the Osaka Prefectural Institute of Public Health, Osaka, Japan [7].

Detection of the virulence genes: STEC O157:H7 Sakai strain was used as a positive control for *eae, iha, efa1* and *ehaA* genes. STEC O113:NM isolated in this study was used as a positive control for *saa, lpfA$_{O113}$, cdt-V* and *subAB* genes. These 4 PCR products were confirmed to be the corresponding genes by sequencing as described previously [10]. *E. coli* strain C600 was used as a negative control. The virulence genes, such as *eae, saa, iha, lpfA$_{O113}$, ehaA, efa1, subAB* etc. were amplified by PCR using primers and conditions as described in Table 1. Each PCR product was purified by QIAquick PCR purification kit (QIAGEN GmbH, Hilden, Germany) and radiolabeled by the random priming method, each ^{32}P-labeled DNA was used as a probe in colony hybridization following the protocol as described above. For *cdt*-gene probe, a mixture of *cdt-IB, cdt-IIIB* and *cdt-IVB* genes specific PCR products which could react with so far identified all 5 types of *cdt* (I to V) was used. The *cdt*-gene positive strains were amplified by PCR using *cdt*-common primer set and were subtyped by PCR-RFLP with *Eco*RI, *Eco*RV and *Msp*I, and by specific PCR for *cdt-V* as described previously [10]. The *eae*-gene positive strains were amplified by PCR using *eae*-F and *eae*-R primer set and were subtyped by PCR-RFLP with *Msp*I as described previously [39].

Pulsed-field Gel Electrophoresis (PFGE): PFGE was performed according to the Centers for Disease Control and Prevention PulseNet USA protocol. Briefly, the isolates grown on tryptic soy agar (TSA) supplemented with 5% defibrinated sheep blood (Nippon Bio-Supp. Center, Tokyo, Japan) for 14-18 hr at 37°C were suspended in cell suspension buffer (100 mM Tris-HCl, 100 mM EDTA [pH 8.0]). Each cell suspension was adjusted to OD_{610} of 1.35. The cell suspension was mixed with 0.5 mg/m*l* proteinase K (P8044-5G, Sigma-Aldrich Co, St Louis, Mo, U.S.A.), and the samples were then mixed with an equal volume of 1% Seakem gold agarose (FMC bioproducts, Rockland, ME, U.S.A.) to make plugs. The bacterial cells were lysed within the plugs by incubation with a lysis solution (50 mM Tris-HCl, 50 mM EDTA [pH 8.0], 1% sarcosine, and 0.1 mg/m*l* of Proteinase K) for 2 hr at 54°C. The plugs were washed twice with distilled water (DW) and 4 times with TE buffer. Cut slices of plugs were equilibrated in restriction enzyme buffer for 20 min at room temperature followed by digestion with 50 U of *Xba*I (Takara Bio Inc., Shiga, Japan) in fresh buffer for 2 hr at 37°C. PFGE was performed with the contour-clamped homogenous electric field method on a CHEF Mapper system (Bio-Rad Laboratories, Hercules, CA. U.S.A.) in 0.5×TBE (45 mM Tris-borate, 1 mM EDTA [pH 8.0]) buffer for 40.24 hr as described previously [42]. Run conditions were generated by the autoalgorithm mode of the CHEF Mapper PFGE system with a size range of 20- to 300-kb. PFGE fingerprints were analyzed by visual inspection according to Tenover's criteria [35], i.e., strains having up to 6 DNA fragments differences were considered to be possibly related and designated as subtypes while strains having 7 or more band differences were considered as distinct types. The representative types and subtypes were further analyzed by Fingerprinting II software (Bio-Rad) to create dendrograms by using the Dice coefficient, the unweighted pair group method with arithmetic means (UPGMA), and a position tolerance of 1.0%.

Quantification of Stx1 and Stx2 toxins by bead-ELISA: Production of Stx1 and Stx2 were quantified by bead-ELISA as described previously [41]. Briefly, STEC strains were cultured in 3 m*l* of TSB at 37°C for 16 hr with shaking (180 rpm). One milliliter of culture was collected and centrifuged at 12,000 × *g* for 10 min. Supernatant (Sup) and bacterial pellet were separated. Bacterial pellet was resuspended in 1 m*l* of PBS and sonicated on ice three times for 1 min each with 1 min interval. Bacterial lysate was centrifuged at 12,000 × *g* for 10 min. Supernatant was collected and used as cell-associated fraction (Cell). Sup and Cell were further filtrated through 0.22 μm filter (IWAKI, Tokyo, Japan) and Stx present in these filtrates was analyzed by bead-ELISA.

Statistical analysis: Statistical analysis of Stx production between cattle and human was performed by Student's *t*-test. A p-value of < 0.05 was considered statistically significant.

RESULTS

Isolation of STEC from diarrheal patients: A total of 35 rectal swab samples out of 1,771 were *stx1* and/or *stx2* gene-positive by multiplex-PCR assay. However, 28 STEC strains from these 35 positive samples were recovered by a colony hybridization assay as described in Materials and Methods. These 28 strains were serologically classified into O157:H7 (n=20), O157:NM (n=1), O26:H11 (n=3), O111:NM (n=1), O91:H21 (n=1), OUT:NM (n=1) and Orough:H21 (n=1) serotypes.

Isolation of STEC from cattle: Three hundred and forty-one *stx1* and/or *stx2* gene-positive strains detected by the colony hybridization assay were isolated from 543 samples and among them 171 *stx1* and/or *stx2* gene-positive strains identified as *E. coli* by biochemical tests were randomly selected for further characterization.

Virulence gene profile: Virulence gene profile including *eaeA, saa, iha, efa1, lpfA$_{O113}$* and *ehaA* genes for adhesions, and toxin genes such as *cdt* and *subAB* were investigated by the colony hybridization assay. Among 171 STEC strains isolated from healthy cattle, *lpfA$_{O113}$, ehaA, iha, saa, cdt* and *subAB* genes were detected in 170 (99%), 163 (95%), 161 (94%), 155 (91%), 112 (65%) and 84 (49%), respectively, while *eaeA* and *efa1* genes were detected in only in 2 (1.2%) strains each (Table 2), respectively. However, among 61 human STEC strains, *ehaA, iha, eaeA* and *efa1* genes were

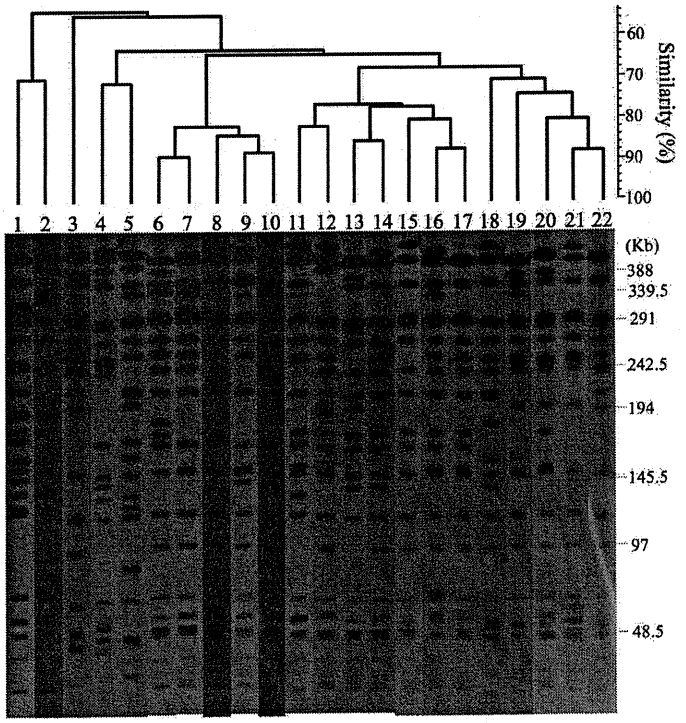

Fig. 1. Dendrogram of *Xba*I-digested representative PFGE patterns (H1 to H22) of STEC O157:H7 strains isolated from patients. Dendrogram was created with the Fingerprinting II software (BioRad Laboratories) by using the Dice coefficient, the unweighted pair group method with arithmetic means (UPGMA), and a position tolerance of 1.0%. The scale above the dendrogram indicates percent similarity. PFGE type and number of isolates are indicated in parenthesis. Lanes 1, P-513 (H1, 2); 2, P-2453 (H2, 2); 3, P-753B (H3, 3); 4, T51 (H4, 1); 5, V-97 (H5, 1); 6, V-17 (H6, 2); 7, EC-1107 (H7, 10); 8, EC-1137 (H8, 1); 9, V-64 (H9, 1); 10, V-66 (H10, 1); 11, V-7 (H11, 1); 12, V-93 (H12, 1); 13, P-563 (H13, 1); 14, V-95 (H14, 3); 15, P-2628 (H15, 2); 16, V-107 (H16, 1); 17, V-252 (H17, 1); 18, V-2 (H18, 1); 19, V-90 (H19, 1); 20, 61279 (H20, 10); 21, P-2666 (H21, 1); 22, V-98 (H22, 1).

detected in 60 (98%), 59 (97%), 58 (95%) and 58 (95%) strains, respectively, while *lpfA*$_{O113}$, *saa*, *cdt* and *subAB* were detected only in 11 (18%), 2 (3.3%), 2 (3.3%) and 1 (1.6%) strains, respectively (Table 3). Type of *cdt* genes was further determined as *cdt-V* in all cases by PCR. The intimin (*eae*) gene was detected in 58 strains (48 of O157, 5 of O111, 4 of O26 and 1 of O145) out of 61 human isolates (95%) and 2 strains (O26 and O111) out of 171 isolated from cattle in this study. Furthermore, intimin type was determined as β in O26:H11 (cattle and human), γ2 in O111:NM (cattle and human) and γ1 in O145 and O157 (human) by PCR-RFLP as shown in Tables 2 and 3.

PFGE: PFGE was employed to investigate genetic diversity of O157 (n=48) and non-O157 (n=13) STEC strains isolated from diarrheal patients. In the case of O157 strains (n=48), 22 PFGE types were identified following Tenover's criteria [35] (Fig. 1). The non-O157 STEC strains (n=13) produced 12 different PFGE types (Fig. 2). As a result, a total of 34 different PFGE types (H-1 to H-34) were recognized among 61 STEC strains (Figs. 1 and 2). The PFGE data analyzed according to Tenover's criteria correlated with 89% cut-off value of dendrogram analyses for individual type differentiation. These data suggest that most of the STEC strains used in this study were genetically diverse.

Production of Stx1 and Stx2: Thirteen STEC strains, one from each cluster (A to M) as shown in Table 2, isolated from healthy cattle and 34 strains isolated from diarrheal patients (Table 3), were examined for Stx1 and Stx2 productions in Sup and Cell fractions, respectively, by bead-ELISA. Stx1 or Stx2 production was compared between cattle and human isolates and is shown in Fig. 3. There were no significant differences in Stx1 production levels between cattle (140 to 250 *n*g/m*l*; in average 190 *n*g/m*l*) and human isolates (130 to 320 *n*g/m*l*; in average 190 *n*g/m*l*). However, there were significant differences in Stx2 production levels between cattle (0 to 220 *n*g/m*l*; in average 100 *n*g/m*l*) and

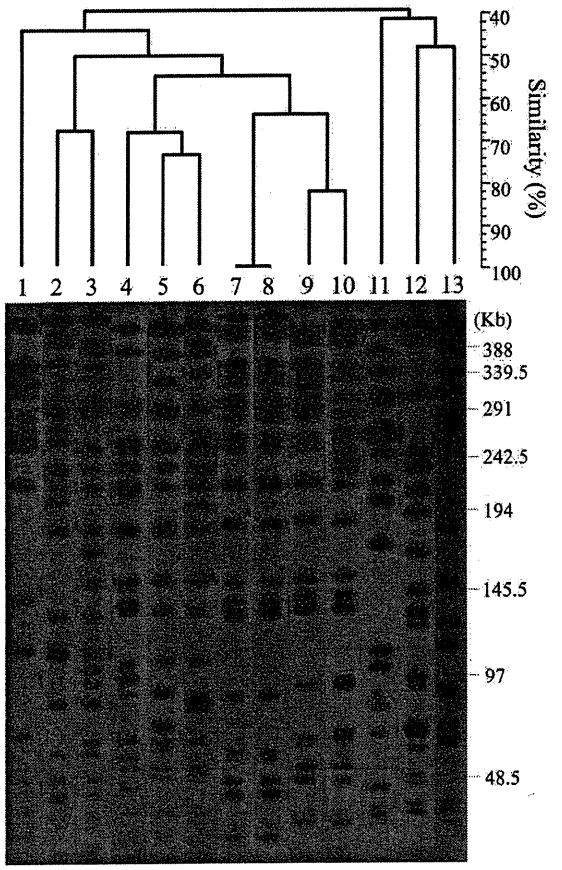

Fig. 2. Dendrogram of *Xba*I-digested PFGE patterns (H23 to H34) of STEC non-O157 strains isolated from patient. Serotype and PFGE type are indicated in parenthesis. Lanes 1, V-8 (O145:NM, H23); 2, P-214 (OUT:NM, H24); 3, P-2681 (O111:NM, H25); 4, V-33 (O26:H11, H26); 5, P-590 (O26:H11, H27); 6, P-658 (O26:H11, H28); 7, P-669 (O26:H11, H28); 8, V-9 (O111:NM, H29); 9, P-650 (Orough:H21, H30); 10, V-32 (O111:NM, H31); 11, V-257 (O111:NM, H32); 12, V-262 (O111:NM, H33); 13, P-2571 (O91:H21, H34).

human isolates (46 to 480 *ng*/m*l*; in average 230 *ng*/m*l*). These data indicate that STEC strains isolated from patients might be more virulent than those isolated from cattle.

DISCUSSION

Among more than 400 serotypes of STEC strains, the O157:H7 serotype is the most predominant among isolates from human patients, in particular with HC and HUS [8, 30]. Most of the STEC O157:H7 isolated from patients contained the LEE pathogenicity island along with the *eae* gene [30]. Apart from STEC O157, non-O157 STEC strains have also been isolated from patients with HUS [1, 28] and various putative adhesins have been identified in LEE-negative and LEE-positive STEC strains [5, 23, 27, 33, 36, 38]. However, little information is available regarding distribution of the virulence related genes in STEC. In this study, therefore, we conducted a comprehensive analysis of the virulence gene profile, including *eae, saa, iha, efa1, lpfA*$_{O113}$ and *ehaA* genes in STEC strains isolated in Japan and compared the results between STEC strains originated from healthy cattle and from diarrheal patients.

The *eae* gene was detected in 58 (95%) strains (4 O26, 5 O111, 1 O145 and 49 O157) out of 61 isolates from diarrheal patients and only in 2 (1.2%) strains (O26 and O111) out of 171 isolates from cattle (Tables 2 and 3). Furthermore, intimin type was determined to be β in O26:H11 (cattle and human), γ2 in O111:NM (cattle and human) and γ1 in O145 and O157 (human). It indicates that STEC O26:H11 and O111:NM isolated from cattle may be the possible source of human infection. The *saa* gene was discovered in a large plasmid present in LEE-negative STEC O113:H21 strain isolated from HUS patient in Australia [27]. In the present study, it was detected in most of the cattle isolates (91%) in addition to 2 isolates (O91:H21 and Orough:H21) from diarrheal patients (Tables 2 and 3). It has been reported that *saa* gene is present in only LEE-negative non-O157 STEC strains so far and more prevalent in cattle isolates rather than human isolates [4, 14, 34]. Our results also support that finding. In addition, the presence of *saa* gene in only 2 strains isolated from patients in the year 2000 but not in 1990s indicates that STEC carrying *saa* gene might be introduced into Japan recently.

Four genes encoding putative adhesins such as Efa1 [23], Iha [33], EhaA [36] and LpfA$_{O113}$ [5] were identified in outside region of the LEE in particular STEC strains. Efa1 was initially identified in STEC O111:H-, which was responsible for adherence to CHO cells [23, 32]. It has been reported that there was strong correlation between presences of *efa1* and *eae* genes [4, 23]. Our data also shows that *efa1* gene was detected in only LEE-positive STEC strains regardless of their origin. The *iha* gene was identified as a novel bacterial adherence-conferring protein homologous to *V. cholerae* iron-regulated gene A (*irgA*) [33]. The results of the present study indicate a large prevalence of *iha* gene in STEC strains irrespective of their origin (97% in human isolates and 94% in cattle isolates). Toma *et al.* [37] suggested that Iha could be a candidate for vaccine development of STEC because of its wide distribution in STEC strains isolated in Argentina, Brazil and Japan (127 of 139 strains, 91%; Tables 2 and 3). In our study, however, *ehaA* gene was most prevalent in STEC strains regardless of serotype, origin and presence of LEE (98% and 95% in human and cattle isolates, respectively), indicating that EhaA might be the best candidate for vaccine development against STEC. EhaA was identified as a novel autotransporter protein of EHEC O157:H7, which is involved in adhesion and biofilm formation [36]. So far distribution of *ehaA* gene has not been analyzed and reported. To our knowledge, this is the first report showing the large-scale occurrence and wide distribution of *ehaA* gene among STEC strains. In STEC

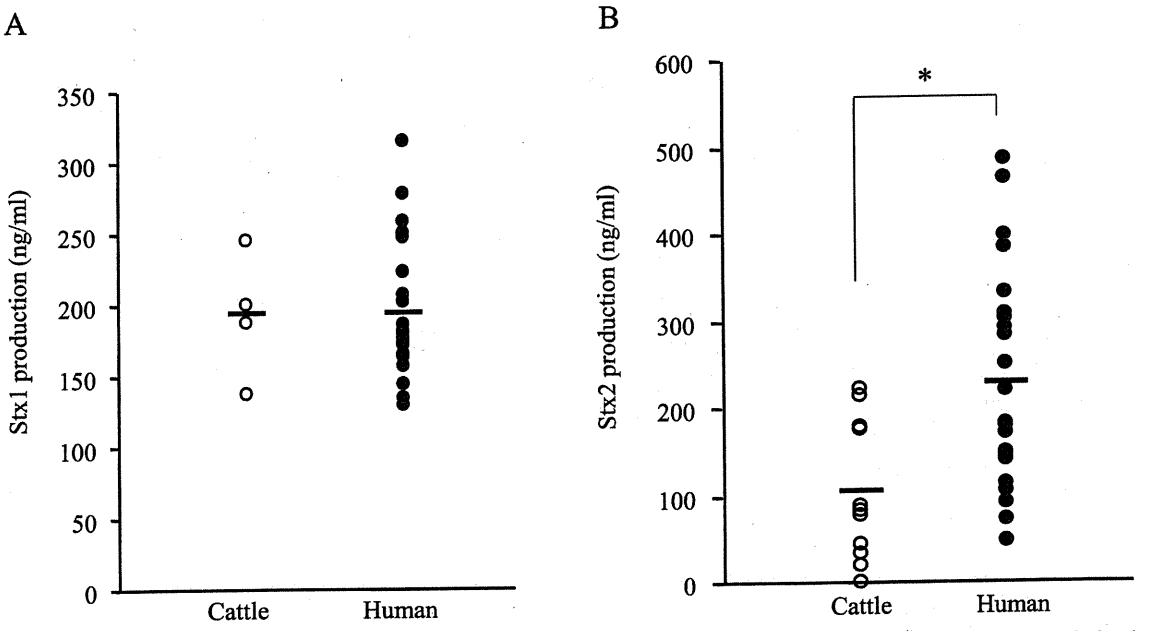

Fig. 3. Detection of Stx1 (A) and Stx2 (B) by bead-ELISA. Open and closed circles indicate Stx production by STEC strains isolated from cattle and human patients, respectively. A bar indicates each average value. *, $p<0.05$ by Student's t-test.

O157:H7, *lpfA* gene was initially identified which was closely related to the long polar (LP) fimbrial (lpf) operon of *Salmonella enterica* serovar Typhimurium [9, 31]. The $lpfA_{O113}$ gene in a novel fimbrial gene cluster was reported in LEE-negative EHEC O113:H21 strain isolated from HUS patient [5]. Osek *et al.* [24] reported that $lpfA_{O113}$ gene was present in only LEE-negative STEC strains. However, $lpfA_{O113}$ gene was detected in LEE-negative and LEE-positive STEC strains except for serogroup O157 in southern America [4, 37]. Our result also indicates a wide distribution of $lpfA_{O113}$ gene in STEC strains regardless of LEE but exceptional for O157 (Tables 2 and 3).

Apart from adhesins, additional toxins besides Stx are also reported to be important virulence factors in STEC. CDT [13] and SubAB [28] were identified as new types of toxin in STEC strains isolated from HUS patients. Although there are at least five types of CDT in *E. coli* [10], CDT-III and CDT-V have been detected in STEC strains [2, 13]. It has been reported that *cdt* in *eae*-negative STEC was significantly more frequent in those from patients with HUS and in those from patients with diarrhea than in those from asymptomatic carriers [2]. Hinenoya *et al.* [11] has already reported that STEC strains isolated from animals contained *cdt-III* and *cdt-V* in Japan. In this study, however, we have observed that not only animal isolates but also human isolates contained *cdt-V* gene (Table 3). To our knowledge, this is the first report showing the presence of *cdt* genes in human STEC isolates in Japan. Another toxin SubAB, discovered as a new type of AB_5 cytotoxin [28], has been detected in various serotypes of LEE-negative STEC strains [4, 15, 29]. Izumiya *et al.* [12] has reported that LEE-negative STEC strains isolated from human and non-human in Japan contained *subAB* genes. The present study also reveals the existence of *subAB* genes in LEE-negative STEC strains isolated from healthy cattle and human patients (Tables 2 and 3). In addition, we report here for the first time about the presence of *subAB* in several STEC serotypes such as O17:H11, O40:HUT, and O130:H24 (Table 2).

It is notable to mention that among putative adhesin genes although *iha* and *ehaA* genes were equally well distributed in animal and human STEC isolates, *saa* and $lpfA_{O113}$ genes were predominant in STEC strains isolated from healthy cattle while *eae* and *efa1* genes were predominant in STEC strains isolated from human patients. Indeed, we have also observed that some of the STEC strains of cattle origin (clusters A, C, D, E, F, and G, Table 2) consisting of similar putative adhesins were predominantly isolated for a long time in a farm (Taguchi, T. *et al.*, unpublished). Taken together, these data indicate that these putative adhesins might determine the host specificity for colonization of STEC strains. Moreover, although there was no significant difference between Stx1 production levels between animal and human isolates, STEC strains from cattle produced less Stx2 indicating their less pathogenic potential in comparison to that of human isolates. It is of interest to mention that between the Stx1 and Stx2, Stx2 was found to be more frequently associated with bloody diarrhea and HUS than Stx1 [30].

In conclusion, to our knowledge, this is the first comprehensive analysis of virulence gene profiles related to puta-

tive adhesins and new toxins recently identified in STEC strains isolated from cattle and patients in Japan. Among virulence genes, *lpfA*$_{O113}$, *ehaA, iha, saa, cdt-V* and *subAB* are prevalent in STEC isolated from healthy cattle while *ehaA, iha, efa1* and *eae* are prevalent in STEC isolated from patients in Japan. These data suggest that *lpfA*$_{O113}$ and *saa* genes in STEC might be associated with colonization of STEC strain to cattle intestine. Although various serotypes of STEC strains were analyzed in this study (Tables 2 and 3), there was no O157:H7 were in cattle isolates and non-O157 was less in human isolates. For a better understanding of the relationship among virulence genes, serotype and host specificity, further studies are required particularly to focus on the distribution of putative adhesin genes and additional toxin genes besides *stx* with various serotypes of diverse STEC strains including O157 as well as non-O157 isolated from cattle and patients.

ACKNOWLEDGMENTS. This study was performed in partial fulfillment of the requirements of a Ph.D. thesis for Y. Wu from Graduate School of Life and Environmental Sciences, Osaka Prefecture University, Osaka, Japan. We thank Dr. Rupak K. Bhadra, Indian Institute of Chemical Biology, Kolkata, India for critically reading the manuscript.

REFERENCE

1. Bettelheim, K. A. 2003. Non-O157 Verotoxin-producing *Escherichia coli*: A problem, paradox, and paradigm. *Exp. Biol. Med.* **228:** 333-344.
2. Bielaszewska, M., Fell, M., Greune, L., Prager, R., Fruth, A., Tschäpe, H., Schmidt, M. A. and Karch, H. 2004. Characterization of cytolethal distending toxin genes and expression in Shiga toxin-producing *Escherichia coli* strains of non-O157 serogroups. *Infect. Immun.* **72**: 1812-1816.
3. Caprioli, A. and Tozzi, A. E. 1998. Epidemiology of Shiga toxin-producing *Escherichia coli* infections in continental Europe, pp. 38-48. *In*: *Escherichia coli* O157:H7 and other Shiga toxin-producing *E. coli* strains (Kaper, J. B. and O'Brien, A. D. eds.), American Society for Microbiology, Washington, D.C.
4. Cergole-Novella, M. C., Nishimura, L. S., Santos, L. F., Irino, K., Vaz, T. M., Bergamini, A. M. M. and Guth, B. E. C. 2007. Distribution of virulence profiles related to new toxins and putative adhesins in Shiga toxin-producing *Escherichia coli* isolated from diverse sources in Brazil. *FEMS Microbiol. Lett.* **274:** 329-334.
5. Doughty, S., Sloan, J., Bennet-Wood, V., Robertson, M., Robins-Browne, R. M. and Hartland, E. 2002. Identification of a novel fimbrial gene related to long polar fimbriae in locus of enterocyte effacement-negative strains of enterohemorrhagic *Escherichia coli*. *Infect. Immun.* **70**: 6761-6769.
6. Elder, R. O., Keen, J. E., Siragusa, G. R., Barkocy-Gallagher, G. A., Koohmaraie, M. and Laegreid, W. W. 2000. Correlation of enterohemorrhagic *Escherichia coli* O157 prevalence in feces, hides, and carcasses of beef cattle during processing. *Proc. Natl. Acad. Sci. U.S.A.* **97**: 2999-3003.
7. Ewing, W. H. 1986. Edwards and Ewing's Identification of *Enterobacteriaceae*, 4th ed, Elsevier, New York.
8. Gyles, C. L. 2007. Shiga toxin-producing *Escherichia coli*: An overview. *J. Anim. Sci.* **85**: E45-E62.
9. Hayashi, T., Makino, K., Ohnishi, M., Kurokawa, K., Ishii, K., Yokoyama, K., Han, C. G., Ohtsubo, E., Nakayama, K., Murata, T., Tanaka, M., Tobe, T., Iida, T., Takami, H., Honda, T., Sasakawa, C., Ogasawara, N., Yasunaga, T., Kuhara, S., Shiba, T., Hattori, M. and Shinagawa, H. 2001. Complete genome sequence of enterohemorrhagic *Escherichia coli* O157:H7 and genomic comparison with a laboratory strain K-12. *DNA Res.* **8**: 47-52.
10. Hinenoya, A., Naigita, A., Ninomiya, K., Asakura, M., Shima, K., Seto, K., Tsukamoto, T., Ramamurthy, T., Faruque, S. M. and Yamasaki, S. 2009. Prevalence and characteristics of cytolethal distending toxin-producing *Escherichia coli* from children with diarrhea in Japan. *Microbiol. Immunol.* **53**: 206-215.
11. Hinenoya, A., Asakura, M., Shima, K., Nishimura, K., Seto, K., Tsukamoto, T. and Yamasaki, S. 2007. Prevalence and characterization of cytolethal distending toxin (CDT)-producing *Escherichia coli* in domestic animals in Japan. p 100. One Hundred Seventh of General Meeting of American Society for Microbiology. Tronto, Canada. Abstract.
12. Izumiya, H., Iyoda, S., Terajima, J., Ohnishi, M., Yamasaki, S. and Watanabe. H. Distribution of the *subA* gene among LEE-negative STEC isolates in Japan. pp. 84-85. 6th International Symposium on Shiga Toxin (Verocytotoxin)-Producing *Escherichia coli* Infections (VTEC 2006).
13. Janka, A., Bielaszewska, M., Dobrindt, U., Greune, L., Schmidt, M. A. and Karch, H. 2003. The cytolethal distending toxin (*cdt*) gene cluster in enterohemorrhagic *Escherichia coli* O157:H- and O157:H7: characterization and evolutionary considerations. *Infect. Immun.* **71**: 3634-3638.
14. Jenkins, C., Perry, N. T., Cheasty, T., Shaw, D. J., Frankel, G., Dougan, G., Gunn, G. J., Smith, H. R., Paton, A. W. and Paton, J. C. 2003. Distribution of the *saa* gene in strains of Shiga toxin-producing *Escherichia coli* of human and bovine origins. *J. Clin. Microbiol.* **41**: 1775-1778.
15. Khaitan, A., Jandhyala, D. M., Thorpe, C. M., Ritchie, J. M. and Paton A. W. 2007. The operon encoding SubAB, a novel cytotoxin, is present in Shiga toxin-producing *Escherichia coli* isolates from the United States. *J. Clin. Microbiol.* **45**: 1374-1375.
16. Kobayashi, H., Shimada, J., Nakazawa, M., Morozumi, T., Pohjanvirta, T., Pelkonen, S. and Yamamoto, K. 2001. Prevalence and characteristics of Shiga toxin-producing *Escherichia coli* from healthy cattle in Japan. *Appl. Environ. Microbiol.* **67**: 484-489.
17. La Ragione, R. M., Best, A., Woodward, M. J. and Wales, A. D. 2009. *Escherichia coli* O157:H7 colonization in small domestic ruminants. *FEMS Microbiol. Rev.* **33**: 394-410.
18. Lopez, E. L., Contrini, M. M. and Rosa, M. F. D. 1998. Epidemiology of Shiga toxin-producing *Escherichia coli* in South America, pp. 30-37. *In*: *Escherichia coli* O157:H7 and other Shiga toxin-producing *E. coli* strains (Kaper, J. B. and O'Brien, A. D. ed.), American Society for Microbiology, Washington, D.C.
19. McDaniel, T. K., Jarvis, K. G., Donnenberg, M. S. and Kaper, J. B. 1995. A genetic locus of enterocyte effacement conserved among diverse enterobacterial pathogens. *Proc. Natl. Acad. Sci. U.S.A.* **92**: 1664-1668.
20. Mead, P. S. 1999. Food-related illness and death in the United States. *Emerg. Infect. Dis.* **5**: 607-625.
21. Michino, H., Araki, K., Minami, S., Takaya, S., Sakai, N., Miyazaki, M., Ono, A. and Yanagawa, H. 1999. Massive out-

break of *Escherichia coli* O157:H7 infection in schoolchildren in Sakai City, Japan, associated with consumption of white radish sprouts. *Am. J. Epidemiol.* **150**: 787-796.

22. National Institute of Infectious Diseases and Tuberculosis and Infectious Diseases Control Division, Ministry of Health, Labor and Welfare 2009. Enterohemorrhagic *Escherichia coli* infection in Japan as of April 2009. *Infect. Agents Surveilance Rep.* **28**: 1'-2'.
23. Nicholls, L., Travis, H. G. and Robins-Browne, R. M. 2000. Identification of a novel genetic locus that is required for vitro adhesion of a clinical isolated of enterohaemorrhagic *Escherichia coli* to epithelial cells. *Mol. Microbiol.* **35**: 275-288.
24. Osek, J., Weiner, M. and Hartland, E. L. 2003. Prevalence of the lpf_{O113} gene cluster among *Escherichia coli* O157 isolates from different sources. *Vet. Microbiol.* **96**: 259-266.
25. Pal, A., Ghosh, S., Ramamurthy, T., Yamasaki, S., Tsukamoto, T. and Bhattacharya, S. K. 1999. Shiga-toxin producing *Escherichia coli* from healthy cattle in a semi-urban community in Calcutta, India. *Indian J. Med. Res.* **110**: 83-85.
26. Paton, A. W., Woodrow, M. C., Doyle, R. M., Lanser, J. A. and Paton, J. C. 1999. Molecular characterization of a Shiga toxigenic *Escherichia coli* O113:H21 strain lacking eae responsible for a cluster of cases of hemolytic-uremic syndrome. *J. Clin. Microbiol.* **37**: 3357-3361.
27. Paton, A. W., Srimanote, P., Woodrow, M. C. and Paton, J. C. 2001. Characterization of Saa, a novel autoagglutinating adhesion produced by locus of enterocyte effacement-negative Shiga-toxigenic *Escherichia coli* strains that are virulent for humans. *Infect. Immun.* 69: 6999-7009.
28. Paton, A. W., Srimanote, P., Talbor, U. M., Wang, H. and Paton, J. C. 2004. A new family of potent AB5 cytotoxins produced by Shiga-toxigenic *Escherichia coli*. *J. Exp. Med.* **200**: 35-46.
29. Paton, A. W. and Paton, J. C. 2005. Multiplex PCR for direction of shiga toxigenic *Escherichia coli* strains producing the novel subtilase cytotoxin. *J. Clin. Microbiol.* **43**: 2944-2947.
30. Paton, J. C. and Paton, A. W. 1998. Pathogenesis and diagnosis of Shiga toxin-producing *Escherichia coli* infections. *Clin. Microbiol. Rev.* **11**: 450-479.
31. Perna, N. T., Plunkett III, G., Burland, V., Mau, B., Glasner, J. D., Rose, D. J., Mayhew, G. F., Evans, P. S., Gregor, J., Kirkpatrick, H. A., Posfai, G., Hackett, J., Klink, S., Boutin, A., Shao, Y., Miller, L., Grotbeck, E. J., Davis, N. W., Lim, A., Dimalanta, E. T., Potamousis, K. D., Apodaca, J., Anantharaman, T. S., Lin, J., Yen, G., Schwartz, D. C., Welch, R. A. and Blattner, F. R. 2001. Genome sequence of enterohaemorrhagic *Escherichia coli* O157:H7. *Nature* **409**: 529-533.
32. Stevens, M. P., Van Diemen, P. M., Frankel, G., Phillips, A. D. and Wallis, T. S.2002. Efa1 influences colonization of the bovine intestine by Shiga toxin-producing *Escherichia coli* serotypes O5 and O111. *Infect. Immun.* **70**: 5158-5166.
33. Tarr, P. I., Bilge, S. S., Vary, J. C., Jelacic, S., Habeeb, R. L. and Ward, T. R. 2000. Iha: a novel *Escherichia coli* O157:H7 adherence-conferring molecule encoded on a recently acquired chromosomal island of conserved structure. *Infect. Immun.* **68**: 1400-1407.
34. Tatarczak, M., Wieczorek, K., Posse, B. and Osek, J. 2005. Identification of putative adhesion genes in shigatoxigenic *Escherichia coli* isolated from different sources. *Vet. Microbiol.* **30**: 77-85.
35. Tenover, F. C., Arbeit, R. D., Goering, R. V., Mickelsen, P. A., Murray, B. E., Persing, D. H. and Swaminathan, B. 1995. Interpreting chromosomal DNA restriction patterns produced by pulsed-field gel electrophoresis: criteria for bacterial strain typing. *J. Clin. Microbiol.* **33**: 2233-2239.
36. Timothy, J. W., Sherlock, O., Rivas, L., Mahajan, A., Beatson, S. A., Torpdahl, M., Webb, R. I., Allsopp, L. P., Gobius, K. S., Gally, D. L. and Schembri, M. A. 2008. EhaA is a novel autotransporter protein of enterohemorrhagic *Escherichia coli* O157:H7 that contributes to adhesion and biofilm formation. *Environ. Microbiol.* **10**: 589-604.
37. Toma, C., Martinez, E. E., Song, T., Miliwebsky, E., Chinen, I., Iyoda, S., Iwanaga, M. and Rivas, M. 2004. Distribution of putative adhesions in different seropathotypes of Shiga toxin-producing *Escherichia coli*. *J. Clin. Microbiol.* **42**: 4937-4946.
38. Torres, A. G., Zhou, X.,and Kaper, J. B. 2005. Adherence of diarrheagenic *Escherichia coli* strains to epithelial cells. *Infect. Immun.* **73**: 18-29.
39. Tramuta, C., Robino, P., Oswald, E. and Nebbia, P. 2008. Identification of intimin alleles in pathogenic *Escherichia coli* by PCR-restriction fragment length polymorphism analysis. *Vet. Res. Commun.* **32**: 1-5.
40. Waters, J. R., Sharp, J. C. M. and Dev, V. J. 1994. Infection caused by *Escherichia coli* O157:H7 in Alberta, Canada, and in Scotland: a five-year review, 1987-1991. *Clin. Infect. Dis.* **19**: 834-843.
41. Yamasaki, S., Lin, Z., Shirai, H., Terai, A., Oku, Y., Ito, H., Ohmura, M. Karasawa, T., Tsukamoto, T., Kurazono, H. and Takeda, Y. 1996. Typing of verotoxins by DNA colony hybridization with poly- and oligonucleotide probes, a bead-enzyme-linked immunosorbent assay, and polymerase chain reaction. *Microbiol. Immunol.* **40**: 345-352.
42. Yamasaki, S., Nair, G. B., Bhattacharya, S. K., Yamamoto, S., Kurazono, H. and Takeda, Y. 1997. Cryptic appearance of a new clone of *Vibrio cholerae* serogroup O1 biotype El Tor in Calcutta, India. *Microbiol. Immunol.* **41**: 1-6.
43. Yamasaki, S. and Takeda, Y. 1997. Enterohemorrhagic *Escherichia coli* O157:H7 episode in Japan with a perspective on Vero toxins (Shiga-like toxins). *J. Toxicol. Toxin Rev.* **16**: 229-240.
44. Zhang, W. L., Kohler, B., Oswald, E., Beutin, L., Karch, H., Morabito, S., Caprioli, A., Suerbaum, S. and Schmidt, H. 2002. Genetic diversity of intimin genes of attaching and effacing *Escherichia coli* strains. *J. Clin. Microbiol.* **40**: 4486-4492.

Cancer Science
The official journal of the Japanese Cancer Association

Modulation of RIP1 ubiquitylation and distribution by MeBS to sensitize cancer cells to tumor necrosis factor α-induced apoptosis

Seungseob Kim,[1,2,4] Nobumichi Ohoka,[1,4] Keiichiro Okuhira,[1] Kimie Sai,[1] Tomoko Nishimaki-Mogami[1] and Mikihiko Naito[1,3]

[1]National Institute of Health Sciences, Tokyo; [2]Graduate School of Frontier Sciences, The University of Tokyo, Chiba, Japan

(Received May 6, 2010/Revised July 20, 2010/Accepted July 22, 2010/Accepted manuscript online July 31, 2010/Article first published online September 3, 2010)

Overexpression of anti-apoptosis protein cIAP1 due to its genetic amplification is found in certain cancers such as esophageal squamous cell carcinoma, hepatocellular carcinoma, cervical cancer and lung cancer, and plays a significant role in resistance to cancer therapy. We previously reported that a class of small molecules represented by (−)-N-[(2S, 3R)-3-amino-2-hydroxy-4-phenyl-butyryl]-L-leucine methyl ester (MeBS) activates auto-ubiquitylation of cIAP1 for proteasomal degradation, and enhances apoptosis of various cancer cells. However, the molecular mechanism of how MeBS sensitizes cancer cells to apoptosis via downregulation of cIAP1 is not well understood. Here, we show that ubiquitylation and distribution of RIP1, a protein ubiquitylated by cIAP1, is modulated by MeBS. Upon tumor necrosis factor (TNF)α stimulation, ubiquitylated RIP1 associates with the TNF-receptor (TNFR) complex, whereas non-ubiquitylated RIP1 associates with caspase8. MeBS reduces the ubiquitylated RIP1 in the TNFR complex and increases non-ubiquitylated RIP1 bound to caspase8. Downregulation of RIP1 by siRNA reduces apoptosis induced by TNFα plus MeBS treatment. These results indicate an important role of RIP1 in apoptosis induced by combined treatment with TNFα and MeBS, suggesting that MeBS sensitizes cancer cells to apoptosis by modulating RIP1 ubiquitylation and distribution. (*Cancer Sci* 2010; 101: 2425–2429)

Inhibitor of apoptosis proteins (IAP) are a family of anti-apoptotic proteins containing one to three baculoviral IAP repeat (BIR) domains, which are frequently overexpressed in cancer cells.[1,2] Certain IAP such as XIAP/hILP/BIRC4, cIAP1/MIHB/hiap-2/BIRC2, cIAP2/MIHC/hiap-1/BIRC3, ML-IAP/Livin/BIRC7 and Apollon/BRUCE/BIRC6 directly interact with and regulate caspases, executioners of apoptosis.[3–7] The BIR domain in the IAP plays an important role in the interaction with caspases.[8,9] These IAP also contain a domain involved in ubiquitin conjugation (really interesting new gene [RING] finger domain or ubiquitin-conjugating enzyme [UBC] domain), and facilitate proteasomal degradation of caspases and IAP.[2,7,10,11]

Among the IAP family members, cIAP1 is regarded as an oncogene[12] and is overexpressed in human cancers, such as esophageal squamous cell carcinoma, hepatocellular carcinoma, cervical cancer and lung cancer, due to its genetic amplification.[13,14] The expression level of cIAP1 significantly correlates with resistance against anti-cancer drugs, such as carboplatin, cisplatin (cDDP), etoposide and cytosine arabinoside, and radiotherapy.[13,15] This evidence suggests that cIAP1 can be a promising target for cancer therapy.

We previously reported that a class of small molecules, represented by MeBS, induces proteasomal degradation of cIAP1, but not of cIAP2 and XIAP, and sensitizes cancer cells to apoptosis.[16] Mechanistic analysis revealed that MeBS directly interacts with the BIR3 domain of cIAP1 and induces RING-mediated auto-ubiquitylation, thereby promoting proteasomal degradation of cIAP1. However, although cIAP1 can regulate caspases, it does not directly inhibit proteolytic activity of caspases, which is highly contrasted by a potent caspase inhibition by XIAP.[17,18] Thus, the molecular mechanism of how MeBS sensitizes cancer cells to apoptosis via downregulation of cIAP1 is not well understood. It was recently reported that IAP antagonists such as AEG40730 induce cIAP1 degradation, reduce RIP1 ubiquitylation and increase the RIP1 association to caspase8 for apoptosis.[19,20]

cIAP1 is present in death receptor complexes, and MeBS sensitizes cancer cells to apoptosis induced by death receptor ligation more markedly than by chemotherapeutic drugs.[16] These observations prompted us to study the mechanism of how MeBS sensitizes cancer cells to apoptosis induced by tumor necrosis factor (TNF)α. In this paper, we show that ubiquitylation and distribution of RIP1, a target protein for cIAP1-mediated ubiquitylation, is modulated by MeBS, which could be involved in the sensitization to apoptosis triggered by TNFα.

Materials and Methods

Reagents. (−)-N-[(2S, 3R)-3-amino-2-hydroxy-4-phenyl-butyryl]-L-leucine methyl ester (MeBS) was kindly supplied by Nippon Kayaku Co. Ltd, (Tokyo, Japan). Antibodies used in this study were: cIAP1, Bad and Bid (R & D Systems, Minneapolis, MN, USA); XIAP, TRADD and caspase8 (MBL, Nagoya, Japan); cFLIP (Alexix Biochemicals, San Diego, CA, USA); caspase3, Bax, Bcl-X, Bcl2, RIP and HSP90 (BD Transduction Laboratories, San Jose, CA, USA); caspase9 (Cell Signaling, Danvers, MA, USA); PARP (Oncogene Science, Cambridge, MA, USA); TNFRI (R & D Systems and Santa Cruz Biotechnology, Santa Cruz, CA, USA); and GAPDH (SantaCruz).

Cell culture, drug treatment and western blot analysis. Human fibrosarcoma HT1080 and monocytic leukemia U937 cells were maintained in RPMI 1640 medium (Nissui Co., Ltd, Tokyo, Japan) containing 10% heat-inactivated fetal bovine serum (FBS) and 100 μg/mL of kanamycin at 37°C in a humidified atmosphere of 5% CO_2. HT1080 cells and U937 cells were treated for 24 h and 6 h, respectively, with MeBS and TNFα. The cells were harvested and lysed in SDS lysis buffer (100 mM Tris–HCl (pH 7.4), 1% sodium dodecyl sulfate, 10% glycerol) and immediately heated at 100°C for 5 min. Cell lysates containing equal amounts of protein were separated by 4–20% gradient polyacrylamide gel electrophoresis, transferred to PVDF membranes (Millipore, Tokyo, Japan), and western blotted using appropriate antibodies. Protein bands were detected using Enhanced Chemiluminescence detection (ECL) kits (GE Healthcare, Tokyo, Japan). For immunoprecipitation, cells were

[3]To whom correspondence should be addressed. E-mail: miki-naito@nihs.go.jp
[4]These authors contributed equally to this work.

doi: 10.1111/j.1349-7006.2010.01697.x

lysed in immunoprecipitation (IP) lysis buffer (10 mM HEPES (pH 7.4), 142.5 mM KCl, 5 mM MgCl2, 1 mM EGTA, 1% NP-40, containing complete mini protease inhibitor cocktail), and immunoprecipitated with antibodies bound to protein G sepharose. The immunoprecipitates were washed with IP lysis buffer and analyzed using western blot.

Cell death assay. HT-1080 cells were cultured overnight in six-well plates and treated with various drugs for 24 h. Floating cells were counted as dead cells, which was confirmed by Trypan blue dye exclusion.[7] U937 cells were fixed and stained with propidium iodide, and apoptotic cells (cells with DNA content less than G1) were quantified in a FACScan flow-cytometer.[21]

RNA interference. The siRNA oligonucleotides corresponding to the sequence of RIP1 (RIP1-1: GCAAAGACCTTACGAGAAT and RIP1-2: CCCAGGGACTCATGATCAT), cIAP1 (TCTAGAGCAGTTGAAGACATCTCTT) and control (TTCTCCGAACGTGTCACGT) were transfected into HT1080 for 48 h using Lipofectamine RNAiMAX (Invitrogen, Tokyo, Japan), and then cells were treated with MeBS and TNFα for 24 h. Floating dead cells were counted as above. The cell lysates were western blotted to confirm downregulation of the proteins.

Results

Sensitization of cancer cells to TNFα-induced apoptosis by MeBS and cycloheximide (CHX). When HT1080 cells were individually treated for 24 h with 20 ng/mL TNFα, 30 μM MeBS or 1 μg/mL CHX, the cells underwent minimal apoptosis. However, the cells underwent extensive apoptosis when cells were treated with 20 ng/mL TNFα in combination with 30 μM MeBS or with 1 μg/mL CHX (Fig. 1A). Similar sensitization was also observed in monocytic leukemia U937 cells (Fig. 1B). U937 cells underwent significant apoptosis when cells were treated with TNFα alone. Co-treatment with MeBS or CHX enhanced the apoptosis of U937 cells, although MeBS or CHX did not induce apoptosis individually. These results indicate that MeBS and CHX sensitize cancer cells to apoptosis induced by TNFα.

Figure 1C shows that MeBS enhanced TNFα-induced apoptosis in a dose-dependent manner. Because higher concentrations of MeBS enhanced apoptosis more markedly and can maintain the reduced cIAP1 level for a longer period of time,[16] we used 30 μM MeBS for most of the experiments in the present study.

TNFα binds to TNFR to assemble death-inducing signaling complex (DISC) for activation of caspase8, an upstream caspase activated by death receptor ligation. To detect caspase activation in the cells, we analyzed the cells using western blot (Fig. 2). Consistent with the extensive apoptosis induced by the combined treatment with TNFα and MeBS, or TNFα and CHX, the precursor form of caspase8 was greatly reduced and cleaved caspase8 appeared in the co-treated cells. In line with this, processing of caspase9 and poly ADP-ribose polymerase (PARP), an indicator of caspase3 activation, were also observed in the cells treated with TNFα plus MeBS and TNFα plus CHX. These results suggest that MeBS and CHX sensitize the cells to apoptosis at a step upstream of caspase8 activation.

MeBS and CHX sensitize cancer cells to TNFα-induced apoptosis by different mechanisms. We studied how MeBS and CHX sensitized cells to TNFα-induced apoptosis. Since MeBS induces auto-ubiquitylation of cIAP1 for proteasomal degradation,[16] we measured the levels of various proteins involved in apoptosis regulation after cells were treated with MeBS and CHX. MeBS reduced the amount of cIAP1 but not XIAP as previously reported (Fig. 3A). Cycloheximide did not affect the amount of IAP, but significantly reduced cFLIP-L protein, another apoptosis-inhibitory protein structurally resembling caspase8,[22] the level of which was not reduced by MeBS. The levels of caspases (caspase3, 8 and 9), pro-apoptotic (Bax, Bad and Bid) and anti-apoptotic (Bcl2 and Bcl-X) Bcl2 family proteins were not changed by MeBS and CHX. Figure 3B shows the reduction of cIAP1 and cFLIP-L by MeBS and CHX, respectively, was evident as early as 1 h after treatment. These results indicate that

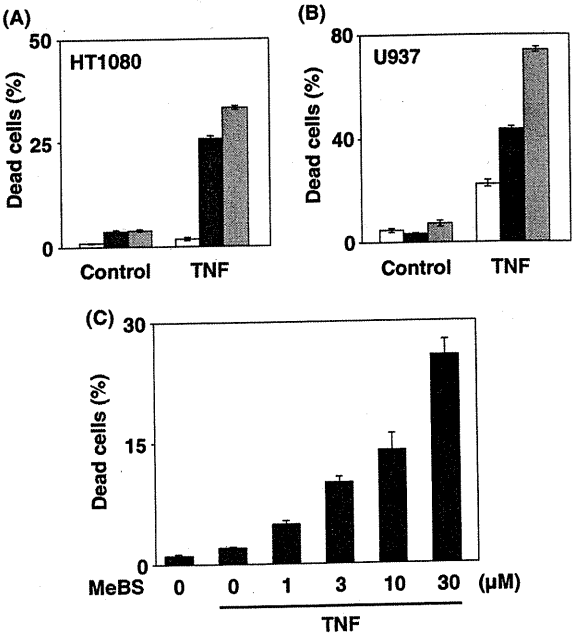

Fig. 1. Enhancement of tumor necrosis factor (TNF)α-induced apoptosis by (–)-N-[(2S, 3R)-3-amino-2-hydroxy-4-phenyl-butyryl]-L-leucine methyl ester (MeBS) and cycloheximide (CHX). HT1080 cells (A) and U937 cells (B) were treated with 20 ng/mL TNFα for 24 or 6 h, respectively, in the absence (white) or presence (black) of 30 μM MeBS and 1 μg/mL CHX (gray). (C) HT1080 cells were treated with 20 ng/mL TNFα with the indicated MeBS for 24 h. Apoptotic cells were counted as described in Materials and Methods. Bars, SD.

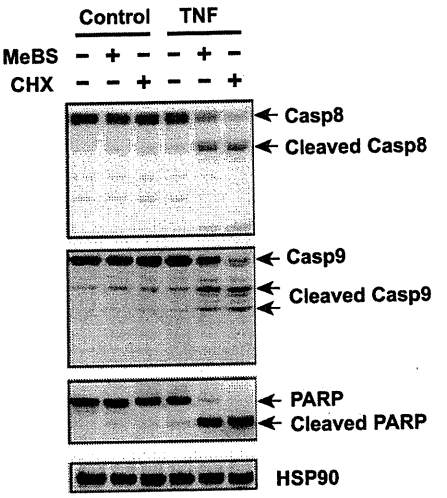

Fig. 2. (–)-N-[(2S, 3R)-3-amino-2-hydroxy-4-phenyl-butyryl]-L-leucine methyl ester (MeBS) and cycloheximide (CHX) enhance tumor necrosis factor (TNF)α-induced caspase activation. U937 cells were treated with TNFα with or without MeBS and CHX, and whole cell lysates were analyzed using western blot with the indicated antibodies.

doi: 10.1111/j.1349-7006.2010.01697.x

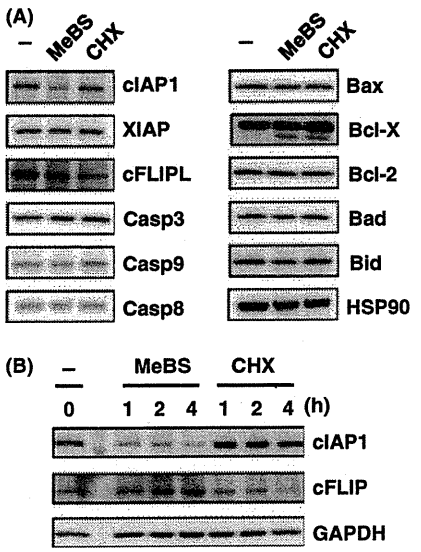

Fig. 3. (–)-N-[(2S, 3R)-3-amino-2-hydroxy-4-phenyl-butyryl]-L-leucine methyl ester (MeBS) reduces cIAP1 whereas cycloheximide (CHX) reduces cFLIP-L. HT1080 cells were treated with MeBS or CHX for 6 h (A) or the indicated time (B), and whole cell lysates were analyzed using western blot with the indicated antibodies.

MeBS and CHX have different mechanisms for sensitization of cancer cells to TNFα-induced apoptosis.

Because cFLIP-L is a close homolog of caspase8 lacking protease activity, and inhibits apoptosis signaling initiated by death receptor ligation, it is likely that CHX sensitizes the cells to TNFα-induced apoptosis by downregulating cFLIP-L. It also indicates that cFLIP-L is a protein with a short half-life compared with other apoptosis regulatory proteins. Hereafter, we focused on the mechanism of how MeBS sensitizes cancer cells to apoptosis via downregulating cIAP1.

RIP1 mediates apoptosis induced by TNFα and MeBS. cIAP1 has a RING domain and ubiquitylates RIP1,[23] and the RIP1 ubiquitylation regulates pro-survival and pro-apoptotic TNF signaling.[24] Therefore, we examined whether RIP1 is involved in the cell death induced by TNFα plus MeBS treatment. When the RIP1 protein level was experimentally reduced by siRNA (Fig. 4A), cell death induced by TNFα plus MeBS was greatly attenuated (Fig. 4B). Consistent with cell death inhibition, caspase8 activation was significantly reduced (Fig. 4C). The loss of cIAP1 by MeBS treatment was not affected by RIP1 depletion (Fig. 4C). These results strongly suggest that RIP1 mediates apoptosis induced by the TNFα plus MeBS treatment.

Change in RIP1 ubiquitylation and distribution by MeBS. When cells are stimulated with TNFα, two signaling complexes are sequentially formed. Complex I includes TNF receptor I (TNFRI), TNFRI-associated death domain protein (TRADD) and TNF receptor-associated factors (TRAFs) to mediate surviving signaling, while complex II (DISC) involves caspase8 for cell death signaling. Because RIP1 associates with both of the complexes, we next investigated the association of RIP1 to the two signaling complexes. RIP1 does not associate with TNFRI in control cells, but it is recruited to complex I upon TNFα treatment (Fig. 5A). The smear and laddering pattern with slower migration of the RIP1 protein band indicates that the RIP1 associated with complex I is mostly ubiquitylated. The ubiquitylation of RIP1 in complex I was reduced by cIAP1 siRNA, while RIP1 association to TNFRI was reduced by RIP1 siRNA (Fig. 5A), which is consistent with the ubiquitylation of RIP1 by cIAP1. Figure 5B shows that MeBS reduced the ubiquitylation

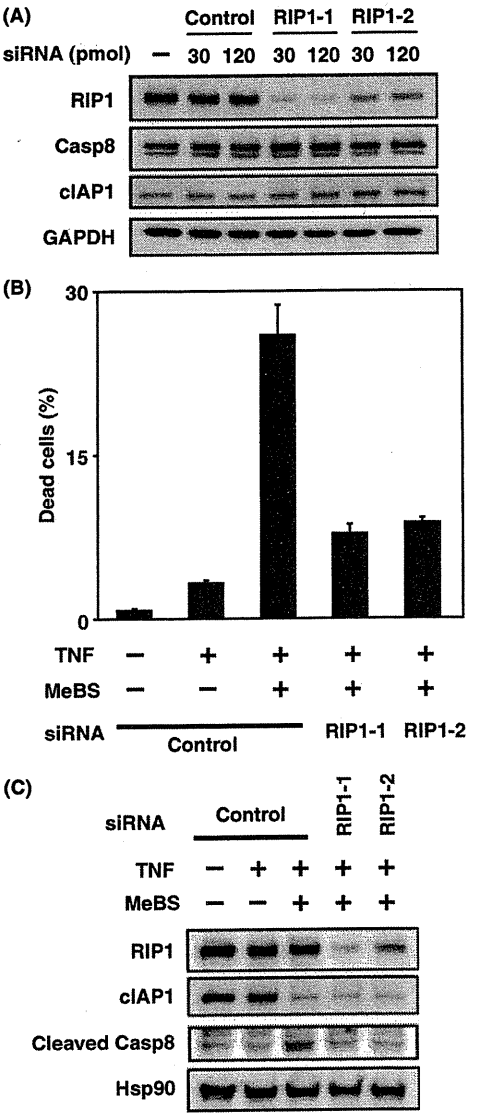

Fig. 4. RIP1 mediates cell death induced by tumor necrosis factor (TNF)α and (–)-N-[(2S, 3R)-3-amino-2-hydroxy-4-phenyl-butyryl]-L-leucine methyl ester (MeBS) treatment. (A) Downregulation of RIP1 protein by small interference RNA. HT1080 cells were transfected with siRNA against RIP1 for 48 h, and cell lysates were analyzed using western blot with the indicated antibodies. (B,C) RIP1 depletion attenuates cell death induced by TNFα and MeBS. The siRNA-treated cells were treated with TNFα and MeBS for 24 h. The dead cells were counted (B) and whole cell lysates were analyzed using western blot with the indicated antibodies (C). Bars, SD.

of RIP1 associated with TNFRI at 5 min, as was observed in cells treated with cIAP1 siRNA. Figure 5B also shows that association of the ubiquitylated RIP1 to complex I is transient. The ubiquitylated RIP1 co-precipitated with TNFRI was abundantly observed 5 min after TNFα treatment, whereas it was totally abrogated after 2 h.

We also examined RIP1 protein in complex II (DISC) by a co-precipitation experiment. Immunoprecipitation of caspase8 showed that RIP1 appeared in the DISC after TNFα treatment for 2 h. The RIP1 protein co-precipitated with caspase8 is discrete and no smear band with slower migration was observed, indicating that the non-ubiquitylated RIP1 protein is in the

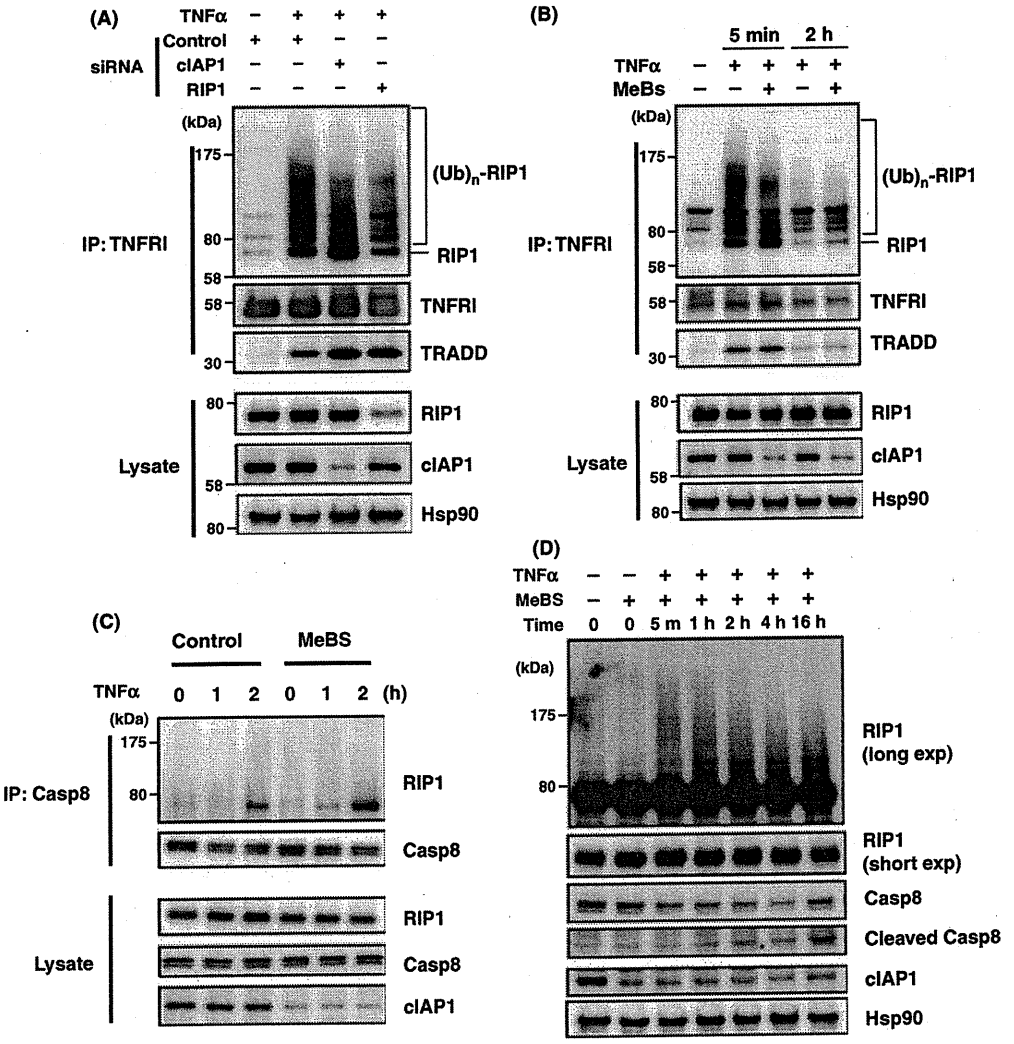

Fig. 5. (–)-N-[(2S, 3R)-3-amino-2-hydroxy-4-phenyl-butyryl]-L-leucine methyl ester (MeBS) modulates ubiquitylation and distribution of RIP1. (A,B) MeBS reduces ubiquitylation of RIP1 associated with TNFRI. (A) HT1080 cells were transfected with siRNA for 48 h and stimulated with TNFα for 5 min. (B) HT1080 cells were pretreated with MeBS for 6 h, and stimulated with TNFα for 5 min and 2 h. Cell lysates were immunoprecipitated with anti-TNFRI and the precipitates were analyzed using western blot with the indicated antibodies. Aliquots of the lysates were analyzed using western blot. (C) MeBS increases non-ubiquitylated RIP1 associated with caspase8. HT1080 cells were pretreated with MeBS for 3 h, and stimulated with TNFα for the indicated times. Cell lysates were immunoprecipitated with anti-caspase8 and the precipitates were analyzed using western blot with the indicated antibodies. (D) HT1080 cells were pretreated with MeBS for 6 h, and stimulated with TNFα for the indicated times. Whole cell lysates were analyzed using western blot with the indicated antibodies. IP, immunoprecipitation; TNF, tumor necrosis factor; TNFRI, TNF receptor I; TRADD, TNFRI-associated death domain protein.

DISC. In the MeBS-treated cells, RIP1 protein began to appear in the DISC at 1 h after TNFα treatment. At 2 h, the amount of RIP1 protein associated with the DISC was larger in the TNFα plus MeBS-treated cells than in the TNFα-treated cells (Fig. 5C). These results indicate that ubiquitylation and distribution of RIP1 is changed by MeBS treatment, which could be involved in the sensitization of cancer cells to apoptosis induced by TNFα.

Figure 5D shows that the RIP1 protein level had not changed for 16 h after the TNFα plus MeBS treatment. The ubiquitylated RIP1 can be found in the whole lysates of cells treated with TNFα plus MeBS for 5 min, and the ubiquitylation appeared to be gradually reduced during the longer incubation time. cIAP1 was kept at a low level for 16 h, and cleaved caspase8 was observed after 16 h when the cells underwent apoptosis.

Discussion

We previously reported that MeBS promotes proteasomal degradation of cIAP1, but not of cIAP2 and XIAP, and sensitizes cancer cells to apoptosis.[16] However, the mechanism of how MeBS sensitizes cancer cells to apoptosis via downregulation of cIAP1 is obscure, since cIAP1 can not directly inhibit the proteolytic activity of caspases,[17] although it can bind to caspase7 and 9.[4] Because cIAP1 associates with death receptor complexes, it is suggested that cIAP1 may regulate apoptosis by influencing signaling pathway triggered by death receptor ligation. In this paper we reported that RIP1, a protein ubiquitylated by cIAP1, mediates apoptosis induced by the TNFα plus MeBS treatment. We also reported that MeBS reduces the ubiquitylated RIP1 protein associated with TNFRI and increases non-ubiquitylated RIP1 bound to caspase8, resulting in an enhanced

doi: 10.1111/j.1349-7006.2010.01697.x

activation of caspase8. Thus, MeBS modulates RIP1 ubiquitylation and distribution, thereby sensitizing cancer cells to apoptosis.

RIP1 was initially identified as a Fas-interacting protein through death domain–death domain interaction.[25] Later studies have indicated that RIP1 is recruited to other death receptors including TNFRI and regulates both surviving and apoptosis signaling.[26] Binding of TNFα to its receptor induces the second formation of two signaling complexes. First, TNFRI recruits RIP1 and TRAF2 in complex I at the plasma membrane. RIP1 is ubiquitylated in complex I, and functions as a scaffold to initiate rapid activation of NFκB signaling leading to the expression of anti-apoptosis proteins such as cFLIP and IAP. Subsequently, complex II (DISC) is formed in which caspase8 or capsase10 is recruited, resulting in an activation of caspases and induction of apoptosis. RIP1 associates with complex II after de-ubiquitylated. Most likely the ubiquitylation of RIP1 in complex I and the subsequent de-ubiquitylation is required for the association of RIP1 with complex II. It was reported that the ubiquitylation state of RIP1 determines whether it functions as a prosurvival scaffold molecule in complex I or a kinase that promotes apoptosis in complex II.[24] Since cIAP1 ubiquitylates RIP1,[23] it is likely that depletion of cIAP1 by MeBS affects the ubiquitylation state of RIP1. In our study, we observed that the ubiquitylation of RIP1 in complex I was reduced in the cells depleted of cIAP1 by siRNA (Fig. 5A) and MeBS (Fig. 5B). However, NFκB signaling is not affected in the MeBS-treated HT1080 cells (data not shown), suggesting that MeBS enhances TNFα-induced apoptosis of this cell line by a mechanism independent of NFκB signaling. The increased association of non-ubiquitylated RIP1 to caspase8 in complex II could be a primary mechanism to enhance apoptosis in the MeBS-treated cells with cIAP1 downregulation. This explanation is supported by the evidence that RIP1 depletion by siRNA attenuates the apoptosis and caspase8 activation by the TNFα plus MeBS treatment (Fig. 4).

Like MeBS, several SMAC mimetic IAP antagonists induce autoubiquitylation and degradation of IAP.[19,20,27,28] Although MeBS is highly specific to cIAP1,[16] some SMAC mimetics target cIAP1, cIAP2 and XIAP for degradation,[19] while others target cIAP1 and cIAP2.[20,27] All of these compounds sensitize cancer cells to TNFα-induced apoptosis, suggesting that cIAP1 is a major target for apoptosis sensitization in terms of TNF signaling. Since cIAP1 is overexpressed in various cancers due to its genetic amplification and cIAP1 expression correlates with resistance to caner therapy,[13–15] targeted destruction of cIAP1 by MeBS and SMAC mimetics is a promising strategy to treat cancers overexpressing cIAP1. When MeBS and SMAC mimetics are provided *in vivo*, circulating TNFα secreted from immune cells or exogenously administered death-inducing ligands might be able to promote apoptosis in cancer cells, which may improve efficacy of anti-cancer therapy.

Acknowledgments

We thank Nippon Kayaku Co. Ltd, for kindly providing MeBS. This study was supported by Grants-in Aid for Cancer Research and Scientific Research from the Ministry of Education, Science, Sports and Culture of Japan.

Disclosure Statement

The authors have no conflict of interest.

References

1 Salvesen GS, Duckett CS. IAP proteins: blocking the road to death's door. *Nat Rev Mol Cell Biol* 2002; **3**: 401–10.
2 Vaux DL, Silke J. IAPs, RINGs and ubiquitylation. *Nat Rev Mol Cell Biol* 2005; **6**: 287–97.
3 Deveraux QL, Takahashi R, Salvesen GS, Reed JC. X-linked IAP is a direct inhibitor of cell-death proteases. *Nature* 1997; **388**: 300–4.
4 Roy N, Deveraux QL, Takahashi R, Salvesen GS, Reed JC. The c-IAP-1 and c-IAP-2 proteins are direct inhibitors of specific caspases. *EMBO J* 1997; **16**: 6914–25.
5 Kasof GM, Gomes BC. Livin, a novel inhibitor of apoptosis protein family member. *J Biol Chem* 2001; **276**: 3238–46.
6 Vucic D, Stennicke HR, Pisabarro MT, Salvesen GS, Dixit VM. ML-IAP, a novel inhibitor of apoptosis that is preferentially expressed in human melanomas. *Curr Biol* 2000; **10**: 1359–66.
7 Hao Y, Sekine K, Kawabata A *et al.* Apollon ubiquitinates SMAC and caspase-9, and has an essential cytoprotection function. *Nat Cell Biol* 2004; **6**: 849–60.
8 Takahashi R, Deveraux Q, Tamm I *et al.* A single BIR domain of XIAP sufficient for inhibiting caspases. *J Biol Chem* 1998; **273**: 7787–90.
9 Srinivasula SM, Hegde R, Saleh A *et al.* A conserved XIAP-interaction motif in caspase-9 and Smac/DIABLO regulates caspase activity and apoptosis. *Nature* 2001; **410**: 112–16.
10 Suzuki Y, Nakabayashi Y, Takahashi R. Ubiquitin-protein ligase activity of X-linked inhibitor of apoptosis protein promotes proteasomal degradation of caspase-3 and enhances its anti-apoptotic effect in Fas-induced cell death. *Proc Natl Acad Sci U S A* 2001; **98**: 8662–7.
11 Yang Y, Fang S, Jensen JP, Weissman AM, Ashwell JD. Ubiquitin protein ligase activity of IAPs and their degradation in proteasomes in response to apoptotic stimuli. *Science* 2000; **288**: 874–7.
12 Zender L, Spector MS, Xue W *et al.* Identification and validation of oncogenes in liver cancer using an integrative oncogenomic approach. *Cell* 2006; **125**: 1253–67.
13 Imoto I, Tsuda H, Hirasawa A *et al.* Expression of cIAP1, a target for 11q22 amplification, correlates with resistance of cervical cancers to radiotherapy. *Cancer Res* 2002; **62**: 4860–6.
14 Imoto I, Yang ZQ, Pimkhaokham A *et al.* Identification of cIAP1 as a candidate target gene within an amplicon at 11q22 in esophageal squamous cell carcinomas. *Cancer Res* 2001; **61**: 6629–34.
15 Tamm I, Kornblau SM, Segall H *et al.* Expression and prognostic significance of IAP-family genes in human cancers and myeloid leukemias. *Clin Cancer Res* 2000; **6**: 1796–803.
16 Sekine K, Takubo K, Kikuchi R *et al.* Small molecules destabilize cIAP1 by activating auto-ubiquitylation. *J Biol Chem* 2008; **283**: 8961–8.
17 Eckelman BP, Salvesen GS. The human anti-apoptotic proteins cIAP1 and cIAP2 bind but do not inhibit caspases. *J Biol Chem* 2006; **281**: 3254–60.
18 Eckelman BP, Salvesen GS, Scott FL. Human inhibitor of apoptosis proteins: why XIAP is the black sheep of the family. *EMBO Rep* 2006; **7**: 988–94.
19 Bertrand MJ, Milutinovic S, Dickson KM *et al.* cIAP1 and cIAP2 facilitate cancer cell survival by functioning as E3 ligases that promote RIP1 ubiquitination. *Mol Cell* 2008; **30**: 689–700.
20 Wang L, Du F, Wang X. TNF-alpha induces two distinct caspase-8 activation pathways. *Cell* 2008; **133**: 693–703.
21 Naito M, Nagashima K, Mashima T, Tsuruo T. Phosphatidylserine externalization is a downstream event of interleukin-1 beta-converting enzyme family protease activation during apoptosis. *Blood* 1997; **89**: 2060–6.
22 Naito M, Katayama R, Ishioka T *et al.* Cellular FLIP inhibits beta-catenin ubiquitylation and enhances Wnt signaling. *Mol Cell Biol* 2004; **24**: 8418–27.
23 Park SM, Yoon JB, Lee TH. Receptor interacting protein is ubiquitinated by cellular inhibitor of apoptosis proteins (c-IAP1 and c-IAP2) *in vitro*. *FEBS Lett* 2004; **566**: 151–6.
24 O'Donnell MA, Legarda-Addison D, Skountzos P, Yeh WC, Ting AT. Ubiquitination of RIP1 regulates an NF-kappaB-independent cell-death switch in TNF signaling. *Curr Biol* 2007; **17**: 418–24.
25 Stanger BZ, Leder P, Lee TH, Kim E, Seed B. RIP: a novel protein containing a death domain that interacts with Fas/APO-1 (CD95) in yeast and causes cell death. *Cell* 1995; **81**: 513–23.
26 Festjens N, Vanden Berghe T, Cornelis S, Vandenabeele P. RIP1, a kinase on the crossroads of a cell's decision to live or die. *Cell Death Differ* 2007; **14**: 400–10.
27 Varfolomeev E, Blankenship JW, Wayson SM *et al.* IAP antagonists induce autoubiquitination of c-IAPs, NF-kappaB activation, and TNFalpha-dependent apoptosis. *Cell* 2007; **131**: 669–81.
28 Vince JE, Wong WW, Khan N *et al.* IAP antagonists target cIAP1 to induce TNFalpha-dependent apoptosis. *Cell* 2007; **131**: 682–93.

J|A|C|S
ARTICLES

Published on Web 04/06/2010

Protein Knockdown Using Methyl Bestatin−Ligand Hybrid Molecules: Design and Synthesis of Inducers of Ubiquitination-Mediated Degradation of Cellular Retinoic Acid-Binding Proteins

Yukihiro Itoh,[†] Minoru Ishikawa,[†] Mikihiko Naito,[‡] and Yuichi Hashimoto*[,†]

Institute of Molecular and Cellular Biosciences, The University of Tokyo, 1-1-1 Yayoi, Bunkyo-ku, Tokyo 113-0032, Japan, and National Institute of Health Sciences, 1-18-1 Kamiyoga, Setagaya-ku, Tokyo 158-8501, Japan

Received January 26, 2010; E-mail: hashimot@iam.u-tokyo.ac.jp

Abstract: Induction of selective degradation of target proteins by small molecules (protein knockdown) would be useful for biological research and treatment of various diseases. To achieve protein knockdown, we utilized the ubiquitin ligase activity of cellular inhibitor of apoptosis protein 1 (cIAP1), which is activated by methyl bestatin (MeBS, **2**). We speculated that formation of an artificial (nonphysiological) complex of cIAP1 and a target protein would be induced by a hybrid molecule consisting of MeBS (**2**) linked to a ligand of the target protein, and this would lead to cIAP1-mediated ubiquitination and subsequent proteasomal degradation of the target protein. To verify this hypothesis, we focused on cellular retinoic acid-binding proteins (CRABP-I and -II) and designed hybrid molecules (compounds **4**) consisting of MeBS (**2**) coupled via spacers of various lengths to *all-trans* retinoic acid (ATRA, **3**), a ligand of CRABPs. Compounds **4** induced selective loss of CRABP-I and -II proteins in cells. We confirmed that **4b** induced formation of a complex of cIAP1 and CRABP-II *in vitro* and induced proteasomal degradation of CRABP-II in cells. When neuroblastoma IMR-32 cells were treated with **4b**, the level of CRABP-II was reduced and cell migration was inhibited, suggesting potential value of CRABP-II-targeting therapy for controlling tumor metastasis. Our results indicate that **4b** possesses sufficient activity, permeability, and stability in cells to be employed in cellular assays. Hybrid molecules such as **4** should be useful not only as chemical tools for studying the biological/physiological functions of CRABPs but also as candidate therapeutic agents targeting CRABPs.

Introduction

Physiological degradation of proteins via the ubiquitin−proteasome system is crucial for regulating cellular functions, including the cell cycle, immunoresponses, and signal transduction.[1] In general, protein ubiquitination or polyubiquitination is mediated by sequential reactions of ubiquitin-activating enzyme (E1), ubiquitin-conjugating enzyme (E2), and ubiquitin ligase (E3). Polyubiquitinated proteins are recognized and degraded by proteasome.[2] Many ubiquitin ligases (E3) have been reported, and it is thought that different E3 ligases have different specificities; i.e., they distinguish various proteins which are to be ubiquitinated.[3] A method for simply and selectively inducing posttranslational degradation of target proteins by regulating this system, which we call protein knockdown, would be useful for biological studies and medical research. It might also provide a new therapeutic strategy in cases where expression of target proteins is closely related to specific diseases.

Genetic techniques such as gene knockout and gene knockdown have been widely used for ablating target proteins and have been useful to uncover the biological functions of numerous proteins in cells or animals. However, complicated and time-consuming genetic manipulation is required for gene knockout. Gene knockdown using RNA interference is an easy method but cannot remove existing proteins and so is especially ineffective in the case of proteins with a long half-life. Therefore, other techniques which can rapidly remove or down-regulate proteins post-translationally would be desirable. One such technique is application of proteolysis-targeting chimeric molecules (protacs)[4] based on peptide structure.[5] Protacs have been reported to degrade target proteins. However, protacs possess peptide structure and must be polyargininated to endow them with sufficient membrane permeability for use in cellular systems.[6] Moreover, stability issues associated with their high molecular weight and vulnerable peptide bonds limit their broad

[†] The University of Tokyo.
[‡] National Institute of Health Sciences.

(1) Konstantinova, I. M.; Tsimokha, A. S.; Mittenberg, A. G. *Int. Rev. Cell Mol. Biol.* **2008**, *267*, 59–124.
(2) Ciechanover, A.; Orian, A.; Schwartz, A. L. *BioEssays* **2000**, *22*, 442–451.
(3) (a) Kee, Y.; Huibregtse, J. M. *Biochem. Biophys. Res. Commun.* **2007**, *354*, 329–333. (b) Deshaies, R. J.; Joazeiro, C. A. *Annu. Rev. Biochem.* **2009**, *78*, 399–434.
(4) (a) Sakamoto, K. M.; Kim, K. B.; Kumagai, A.; Mercurio, F.; Crews, C. M.; Deshaies, R. J. *Proc. Natl. Acad. Sci. U.S.A.* **2001**, *98*, 8554–8559. (b) Sakamoto, K. M.; Kim, K. B.; Verma, R.; Ransick, A.; Stein, B.; Crews, C. M.; Deshaies, R. J. *Mol. Cell. Proteomics* **2003**, *2*, 1350–1358. (c) Schneekloth, A. R.; Pucheault, M.; Tae, H. S.; Crews, C. M. *Bioorg. Med. Chem. Lett.* **2008**, *18*, 5904–5908.

10.1021/ja100691p

Scheme 1. (a) cIAP1 Induces Degradation of Binding Proteins. (b) Auto-Ubiquitination and Degradation of cIAP1. (c) Protein Knockdown Strategy

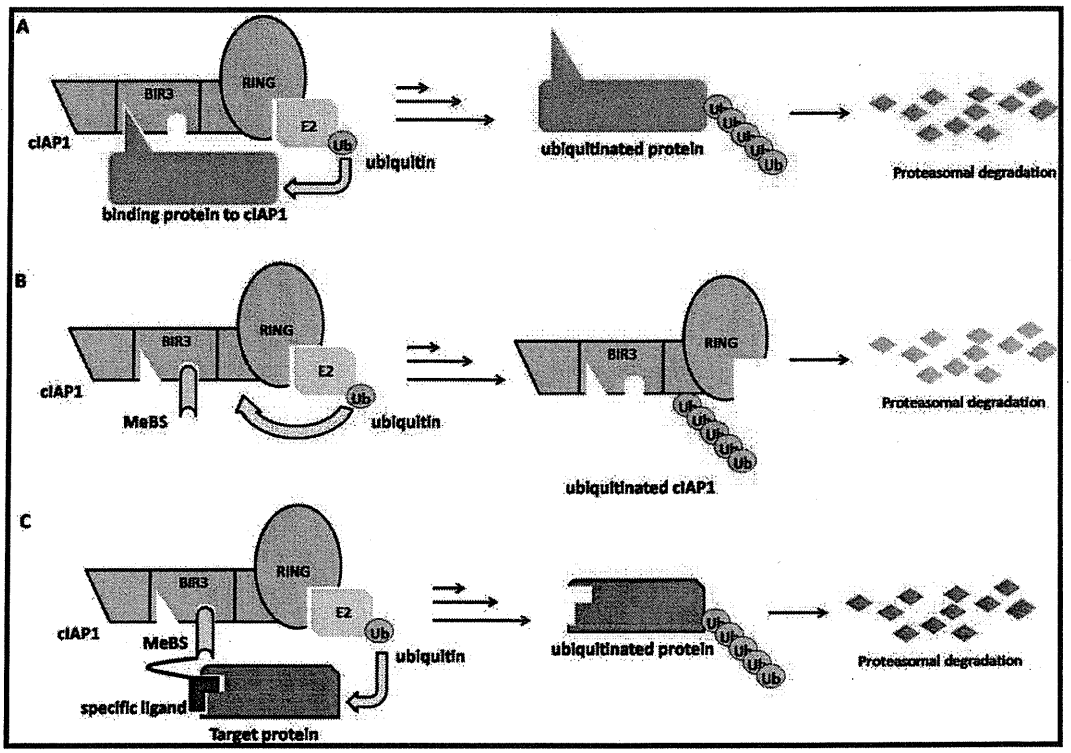

applicability, and other general methods to remove target proteins post-translationally in cells and animals would be desirable. Therefore, we attempted to develop a new approach, which we call protein knockdown, using small molecules to induce selective degradation of target proteins post-translationally.

To develop such a protein knockdown approach, we focused on cellular inhibitor of apoptosis protein 1 (cIAP1), which is one of the inhibitor of apoptosis proteins (IAPs) and is overexpressed in certain tumor cells.[7] It inhibits apoptosis induced by a variety of stimuli.[8] cIAP1 contains (i) three baculoviral IAP repeat (BIR) domains which interact with its binding proteins, including caspases, and (ii) one really interesting new gene (RING) finger domain involved in ubiquitin ligase activity.[7–9] cIAP1 promotes ubiquitination and proteasomal degradation of its binding proteins (Scheme 1a).[9] Furthermore, Naito's group reported that a class of bestatin ester analogues represented by methyl bestatin (MeBS, **2**) bind to the BIR3 domain of cIAP1 and promote autoubiquitination and degradation of cIAP1 (Scheme 1b).[10] Based on these observations, we hypothesized that a hybrid molecule consisting of MeBS (**2**) coupled to a ligand for a target protein might be able to induce cIAP1-mediated ubiquitination and proteasomal degradation of the target protein.

For a proof-of-concept study, we chose cellular retinoic acid binding proteins (CRABP-I and -II) as target proteins. These proteins reside in cytoplasm and specifically bind to *all-trans* retinoic acid (ATRA, **3**), an endogenous ligand of retinoic acid receptors (RARs).[11] CRABP-I is thought to be related to metabolism of retinoic acid (RA) and resistance to RA in cancer cells,[12] while CRABP-II is suggested to be associated with nuclear transportation of RA.[13] It has also been reported that

(5) A non-peptide protac, utilizing murine double minute 2 (MDM2) as an E3 ligase and a non-peptide ligand (nutlin-3) as a MDM2 ligand, degraded androgen receptor (AR) (ref 4c). However, MDM2 naturally induces ubiquitination of AR when Nutlin-3 binds to MDM2. Gaughan, L.; Logan, I. R.; Neal, D. E.; Robson, C. N. *Nucleic Acids Res.* **2005**, *33*, 13–26. Logan, I. R.; McNeill, H. V.; Cook, S.; Lu, X.; Lunec, J.; Robson, C. N. *Prostate* **2007**, *67*, 900–906. Therefore, additional data to compare AR levels with nutlin-3 treatment and protac treatment would be needed to determine whether the decrease of AR is associated with the nutlin-3 derivative or the protac.

(6) (a) Schneekloth, J. S.; Fonseca, F. M.; Koldobskiy, M.; Mandal, A.; Deshaies, R.; Sakamoto, K. M.; Crews, C. M. *J. Am. Chem. Soc.* **2004**, *126*, 3748–3754. (b) Rodriguez-Gonzalez, A.; Cyrus, K.; Salcius, M.; Kim, K.; Crews, C. M.; Deshaies, R. J.; Sakamoto, K. M. *Oncogene* **2008**, *27*, 7201–7211. (c) Lee, H.; Puppala, D.; Choi, E. Y.; Swanson, H.; Kim, K. B. *ChemBioChem* **2007**, *8*, 2058–2062. (d) Puppala, D.; Lee, H.; Kim, K. B.; Swanson, H. I. *Mol. Pharmacol.* **2008**, *73*, 1064–1071. (e) Tang, Y. Q.; Han, B. M.; Yao, X. Q.; Hong, Y.; Wang, Y.; Zhao, F. J.; Yu, S. Q.; Sun, X. W.; Xia, S. J. *Asian J. Androl.* **2009**, *11*, 119–126.

(7) (a) Deveraux, Q. L.; Reed, J. C. *Genes Dev.* **1999**, *13*, 239–252. (b) Salvesen, G. S.; Duckett, C. S. *Nat. Rev. Mol. Cell Biol.* **2002**, *3*, 401–410.

(8) Roy, N.; Deveraux, Q. L.; Takahashi, R.; Salvesen, G. S.; Reed, J. C. *EMBO J.* **1997**, *16*, 6914–6925.

(9) Vaux, D. L.; Silke, J. *Nat. Rev. Mol. Cell. Biol.* **2005**, *6*, 287–297.

(10) (a) Sekine, K.; Takubo, K.; Kikuchi, R.; Nishimoto, M.; Kitagawa, M.; Abe, F.; Nishikawa, K.; Tsuruo, T.; Naito, M. *J. Biol. Chem.* **2008**, *283*, 8961–8968. (b) Sato, S.; Aoyama, H.; Miyachi, H.; Naito, M.; Hashimoto, Y. *Bioorg. Med. Chem. Lett.* **2008**, *18*, 3354–3358.

(11) (a) Donovan, M.; Olofsson, B.; Gustafson, A. L.; Dencker, L.; Eriksson, U. *J. Steroid Biochem. Mol. Biol.* **1995**, *53*, 459–465. (b) Fogh, K.; Voorhees, J. J.; Aström, A. *Arch. Biochem. Biophys.* **1993**, *300*, 751–755.

(12) (a) Fiorella, P. D.; Napoli, J. L. *J. Biol. Chem.* **1991**, *266*, 16572–16579. (b) Kizaki, M.; Ueno, H.; Matsushita, H.; Takayama, N.; Muto, A.; Awaya, N.; Ikeda, Y. *Leuk. Lymphoma* **1997**, *25*, 427–434.

(13) (a) Schug, T. T.; Berry, D. C.; Toshkov, I. A.; Cheng, L.; Nikitin, A. Y.; Noy, N. *Proc. Natl. Acad. Sci. U.S.A.* **2008**, *105*, 7546–7551. (b) Schug, T. T.; Berry, D. C.; Shaw, N. S.; Travis, S. N.; Noy, N. *Cell* **2007**, *129*, 723–733. (c) Budhu, A. S.; Noy, N. *Mol. Cell. Biol.* **2002**, *22*, 2632–2641.